PHENIX Beam Use Proposal
for RHIC Run-11 and Run-12
June 1, 2010

The PHENIX Collaboration

1 Summary

The PHENIX Collaboration proposes a scientific program of precision measurements to pursue key goals in the study of heavy ion collisions and the spin of the proton at RHIC. Our overarching goals are to quantify the properties of the perfect QCD liquid, discover the conditions under which those properties are first manifested, and continue the search for evidence of the QCD critical end point. The RHIC Spin program seeks to answer the puzzle of how the nucleon's half integer spin is carried by its partonic constituents and gain insight on the dynamical nature and correlation amongst the partons in the nucleon.

The PHENIX detector was optimized for precision measurements of rare probes of partonic matter and polarized protons, with particular focus on hard and electromagnetic probes. PHENIX possesses selective triggers, high rate capability, and multiple fast detector systems to track and identify particles. PHENIX is currently in the midst of an ambitious upgrade program. The new silicon microvertex barrel detector (VTX) will be installed in fall 2010, in place of the hadron blind detector. The secondary vertex finding capabilities will be extended by the forward vertex detector (FVTX) in 2012. The new muon trigger system, comprised of upgraded muon tracker front end electronics (MuTr FEE), new resistive plate chambers (RPC's) for timing measurements, and a carefully designed absorber to optimize signal to background, provides trigger capability for W bosons decaying to single muons at forward rapidity. In 2011 we will have triggering in both arms; the background rejection will be further enhanced in 2012 when installation of station 1 RPC's in each arm is complete. We are currently reviewing the design of a forward calorimeter (FOCAL) to measure neutral pions and photons. Furthermore, we have begun a comprehensive review of what has been learned thus far and what key questions are best answered by continued data taking at RHIC. The PHENIX collaboration is in the midst of designing a decadal plan, laying out a path of upgrades to address the most compelling questions. We will exploit the unique capabilities afforded by the flexibility and running time of the dedicated RHIC facility to answer questions that are complementary, or even inaccessible, to the anticipated heavy ion running at the Large Hadron Collider.

In the coming two runs, PHENIX seeks to reap the benefits of the investment in upgrades of the detector as well as improved capabilities of the RHIC complex. Our program with polarized proton collisions at 500 GeV with the new muon trigger will

provide a first look at the flavor dependent anti-quark polarization and extend the x range of sensitivity to gluon polarization. This requires polarized 500 GeV p+p collisions in both runs. Full energy Au+Au collisions in 2011 and 2012 will open a new era in heavy quark spectroscopy by separation of c and b quarks using the new vertex detectors. This will show whether the astounding energy loss of charm quarks in the hot, dense QCD medium extends also to the even heavier b quarks. Furthermore, the increased luminosity afforded by stochastic cooling will allow extending the kinematic range of pion, direct photon, quarkonia, and photon-jet correlation probes. Combining two or more Au+Au data sets taken at high luminosity will further enhance the reach of these measurements.

A new goal, begun in Run-10, is examination of lower energy Au+Au collisions to search for signals of the critical point of the QCD phase transition. The PHENIX Collaboration is excited by the discovery potential at energies between that of the SPS and top RHIC energy. Our goals include the search for onset of perfect liquid flow (i.e. that characteristic of very low viscosity to entropy ratio) by testing the constituent quark scaling of elliptic flow. We will also study the energy dependence of jet quenching to search for the onset of the large opacity associated with strongly coupled quark gluon plasma. Completing this program requires data taking at additional Au+Au energies, and collecting reference p+p data at the same energies as the Au+Au measurements.

The new EBIS source will make it possible, for the first time, to study collisions of highly deformed nuclei and reach higher energy densities than previously available. PHENIX aims to make first measurements of U+U collisions in order to study techniques for selection and control of the collision geometry.

The priorities for the PHENIX Collaboration in Runs-11-12 are:

1. Sample 150 pb^{-1} of 500 GeV polarized p+p collisions; we request 50 pb^{-1} in Run-11 and 100 pb^{-1} in Run-12. This can be accomplished in 10 and 8 weeks, respectively. We believe it is cruicial for the success of the physics program that p+p be run as the first species in both runs to allow commissioning of new detectors with low multiplicity collisions.

2. Full energy Au+Au collisions for the heavy quark physics program with the new vertex detectors. We request 8 weeks in Run-11 and 7 weeks in Run-12.

3. Completion of the energy scan between full and SPS energies. This has two components - one is several weeks devoted to Au+Au collisions at 27 and 18 GeV. The other is several weeks of low energy, unpolarized p+p reference collisions at 62.4,39, 27 and 22.4 GeV. We anticipate completing the first component of this program in Run-11 and the second in Run-12.

4. A first look at U+U collisions, utilizing the new EBIS source.

This document is organized as follows: Section 2 provides an introduction. Section 3 presents recent PHENIX achievements relevant to the program proposed for Run-10 last year and the future program presented in this document; this includes discussion of data collected and detector performance in Run-10, as well as key physics results of direct relevance to this proposal. Section 4 discusses the status of the PHENIX Experiment, including upgrades installed for Run-11 and those underway for use in the future. Section 5 is the Beam Use Proposal for Runs 11 and 12; it outlines our assumptions and presents projected sensitivities for the physics driving the proposed running time.

2 Introduction

The physics goals of the PHENIX Collaboration for RHIC running have evolved with increasing knowledge, higher luminosities, and improved detection capabilities [1, 2, 3, 4, 5, 6, 7, 8, 9, 10, 11, 12]. The consistent theme is the need for the highest possible integrated luminosities (and polarizations in the case of p+p running) to explore fully the range of fundamental phenomena in nucleus+nucleus, "proton"+nucleus and proton+proton collisions. PHENIX utilizes selective triggers, high rate capability, and multiple fast detector systems to track and identify particles. Over the past years, PHENIX triggering, data acquisition, archiving, and data analysis have kept up with incremental RHIC accelerator improvements. In fact, data from Run-10 are currently being reconstructed; production is already done for the lower energy data. We successfully provide timely data analysis using the RHIC Computing Facility (RCF), and also computing resources at PHENIX collaborating institutions, particularly in Japan ("CC-J") and France ("CC-F").

PHENIX is currently undertaking an ambitious upgrade program. A major upgrade for triggering on high momentum muons from W decays is ready for data taking in 2011. Beginning in fall 2010, the new silicon microvertex barrel detector (VTX) will be available, replacing the Hadron Blind Detector (HBD). In 2012, the microvertex capabilities will be extended by the forward vertex detector (FVTX). We have a design in hand for a forward calorimeter (FOCAL) to trigger on neutral pions and photons, and provide coincidence measurements with particles detected in the existing high resolution midrapidity detectors. We look forward to using these detectors and the increased luminosity afforded by stochastic cooling of heavy ion beams and electron lenses for proton beams. We aim to investigate the proton spin, the gluon structure of the nucleus, and properties of hot, dense partonic matter with rare probes such as energetic jets and b quarks that have been previously unavailable at RHIC.

PHENIX has made significant progress in both the heavy ion and the spin programs. However, the curtailed running time and limits on p+p collision luminosity have adversely affected the spin program. Although the 2009 exploratory run at 500 GeV was very successful, the overall polarized proton performance in Run-9 underscores the deleterious

impact that lack of polarized p+p running has upon polarization and luminosity development. Polarization is a key factor in the figure of merit for the spin physics goals, and the expected polarization levels have not yet been attained. This significantly slows progress toward the goals laid out in the RHIC Spin Research plans[13, 14].

We present in this Beam Use Proposal a plan for the next two years that takes optimum advantage of the exciting PHENIX upgrades and RHIC luminosity increases in both p+p and Au+Au running. We will utilize the new muon trigger capabilities to make first measurements of W asymmetry at forward rapidity, and the silicon microvertex detectors to separate D and B mesons in heavy ion collisions to determine whether the b quark energy loss is as remarkably large as that of c quarks. In addition, the large acceptance afforded by the barrel VTX will greatly increase the acceptance for hadrons and jets, opening a new era for jet probes of the quark gluon plasma in PHENIX.

3 Recent PHENIX Achievements

The PHENIX Collaboration has continued the tradition of simultaneously collecting and analyzing data, publishing exciting physics results, and planning and constructing detector upgrades. Between mid-2009 and the present time, PHENIX submitted ten new papers for publication. This includes 5 archival papers that are several tens of pages in length. There are 6 papers on heavy ion collisions, 3 on non-polarized observables in p+p collisions, and one new spin physics result.

3.1 Successful Data Taking in Run-10

The central arm configuration of PHENIX from Run-8 through Run-10 is shown in Figure 1. The red circles indicate detectors installed in the first round of PHENIX upgrades. The Hadron Blind Detector will be removed shortly, and will be replaced by the Silicon Microvertex detector (VTX).

Figure 2 shows the RPC Station 3 detectors, which were successfully installed in the North muon arm during the shutdown prior to Run-10. The installation schedule was extraordinarily aggressive, and the tight quarters in the location of the detectors made the installation extremely challenging. Production of all RPC detector modules for the South arm muon trigger has been completed, and installation will take place during the 2010 shutdown of RHIC.

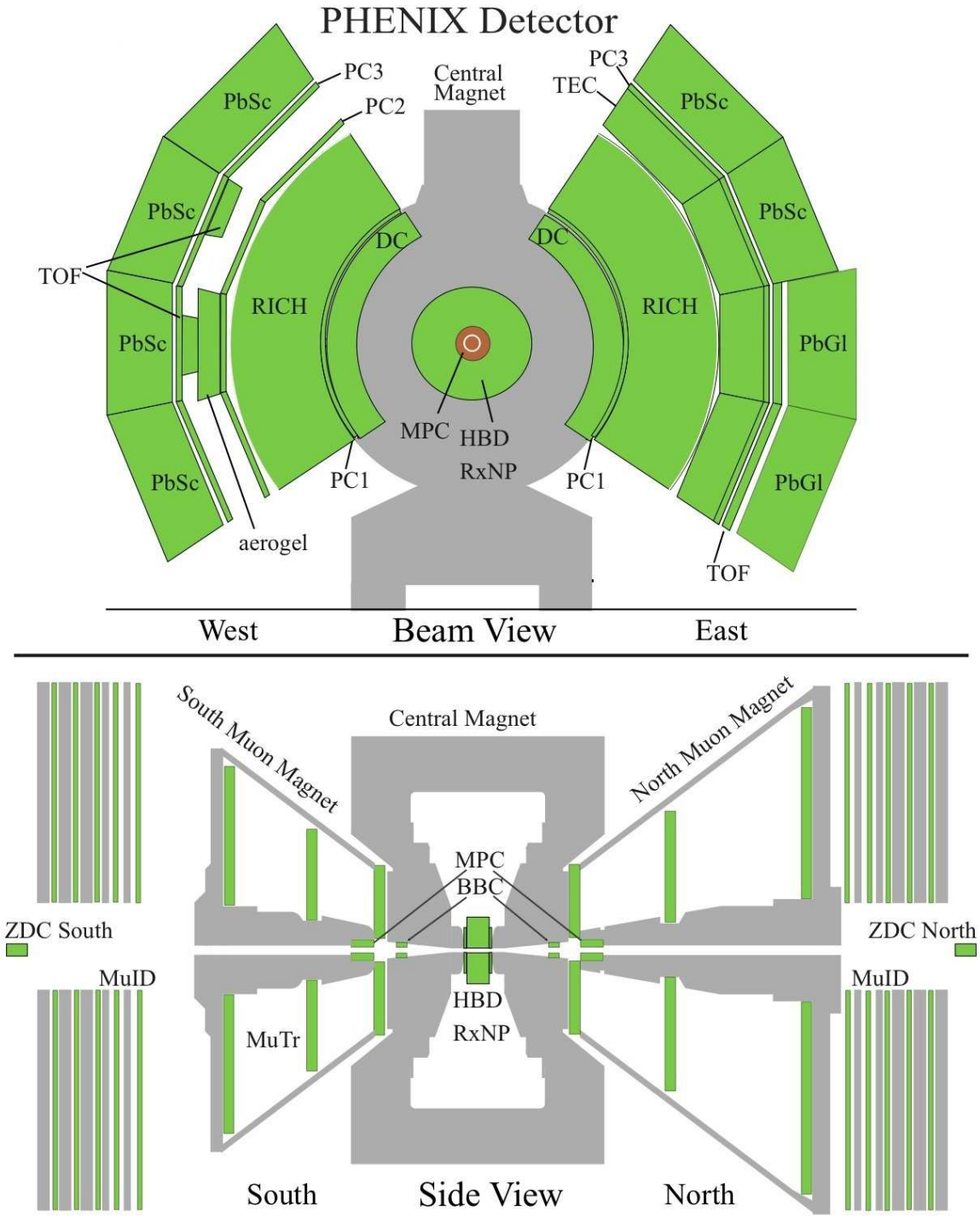

Figure 1: Configuration of PHENIX from 2008. The VTX will surround a new, smaller Be beampipe.

Figure 2: Installed RPC Detector for North muon trigger.

Table 1: PHENIX Data Sets in Run-10

SPECIES	$\sqrt{s_{NN}}$	Requested	Recorded	Recorded (events)	Data size
Au+Au	200	1.4 nb^{-1}	1.3 nb^{-1}	8.2G	885 TB
Au+Au	62.4	350M events	0.11 nb^{-1}	700M	76 TB
Au+Au	39	50M events	40 μb^{-1}	250M	34 TB
Au+Au	7.7		0.26 μb^{-1}	1.6M	6 TB

3.1.1 PHENIX performance in Run-10

In Run-10, PHENIX carried out a near-realtime reconstruction of data in the counting house. For 200 GeV Au+Au, we reconstructed a subset of peripheral collisions, primarily for diagnostics on HBD performance. At 62.4 and 39 GeV, we were able to reconstruct a significant fraction of the entire data sets. At 7.7 GeV the data rate was a few Hz, so reconstruction of all events was performed in real-time as part of data monitoring in the counting house.

The Hadron Blind Detector operated stably during the entire duration of Run-10. The run began with $\approx 95\%$ operational detector channels; the missing 5% was due to one problematic module which was ultimately disabled. The detector readout was successfully operated with fewer samples read out than in Run-9.

First analysis of Hadron Blind Detector data in full energy Au+Au collisions indicates that the HBD performed in Run-10 as well as in Run-9. Figure 3 shows the position difference between HBD clusters and track projections into the HBD in peripheral Au+Au

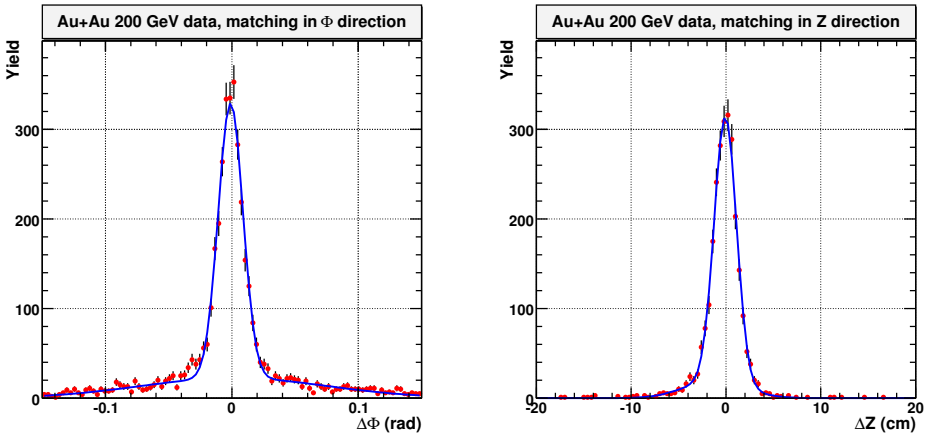

Figure 3: Track matching residuals in the azimuthal (ϕ, left) and beam (z, right) directions, illustrating good cluster position resolution in the HBD for Au+Au collisions.

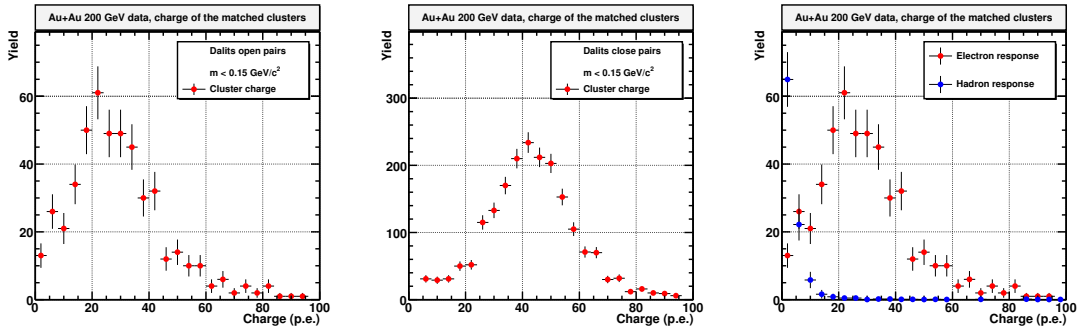

Figure 4: Left: Run-10 HBD response to single electrons. Center: Run-10 HBD response to double electrons. Right: Electron-hadron separation performance in peripheral Au+Au collision data.

collisions. The performance is essentially the same as in Run-9, with good position resolution. The number of photoelectrons for single and double electrons are also very similar to that in Run-9, with peaks as 20 and 40 photoelectrons as shown in Figure 4. The figure also illustrates good electron-hadron separation in peripheral Au+Au. Single vs double electron separation is being tuned for high multiplicity events. Electron detection efficiency and combinatorial background rejection determination require a larger number of reconstructed events than those currently in hand. We expect to begin full reconstruction of the 62 GeV Au+Au data set shortly, which will allow to quantify the HBD performance fully.

The superb performance of RHIC in Run-10 allowed PHENIX to collect over 8 billion events at 200 GeV and 700 million events in 62.4 GeV Au+Au collisions. This will allow excellent measurement of the low mass dilepton spectrum, and also to determine whether

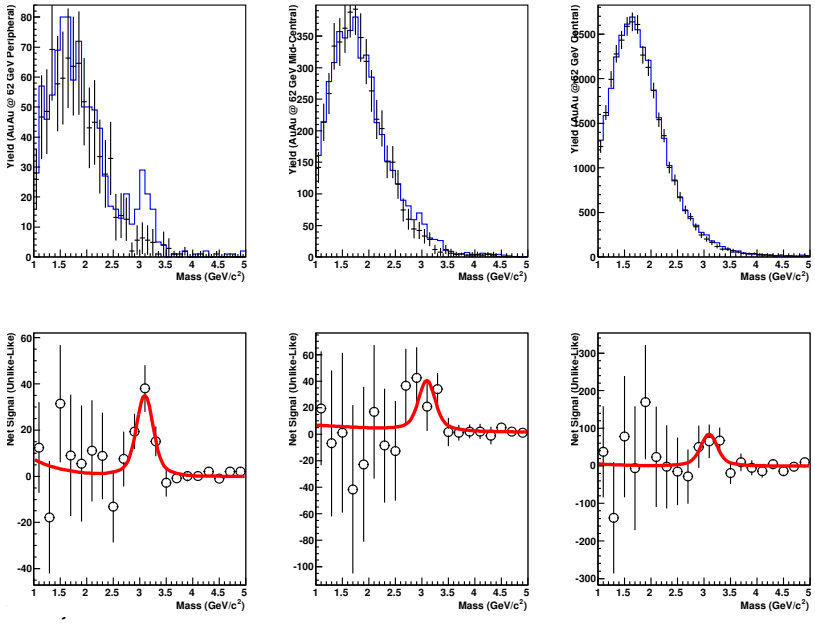

Figure 5: Dimuon invariant mass spectra in peripheral, mid-central and central 62.4 GeV Au+Au collisions. Top panels show unlike-sign (blue) and like-sign (black) spectra. Bottom panels show like-sign subtracted mass spectra.

the large excess already observed by PHENIX at 200 GeV persists to lower $\sqrt{s}$. Because the data set is so large, rare probes of the plasma also come within reach. Figure 5 shows a first look at J/ψ production in 62.4 GeV Au+Au collisions, measured via the dimuon decay channel. This analysis was carried out on 1/4 of the full data set, i.e. about 175 million events. The top panels show the mass distribution of all opposite sign (blue) and like sign (black) dimuons, while the lower panels show the mass distribution of unlike sign dimuons after like sign subtraction; J/ψ peaks are clearly visible. The data quality will obviously improve due to muon arm detector alignment and final calibration, utilization of the full data set, and subtraction of dimuons from mixed events in place of like-sign subtraction.

In the 39 GeV Au+Au run, PHENIX collected 250 million events. With such a data sample, which is substantially larger than initially anticipated, it should be feasible to measure the low mass dielectron spectrum at a third energy. The data collection finished only a few weeks ago, so the data analysis has not yet been done. However, the expected performance was scaled from careful projections at 200 GeV. The invariant mass distribution with expected error bars is shown in Figure 6. The figure shows that for a low mass excess around 200-500 MeV/c^2 down to three times smaller than that observed at 200 GeV, we would still have a significant result.

PHENIX took first production data at sub-injection energy in Run-10. Careful com-

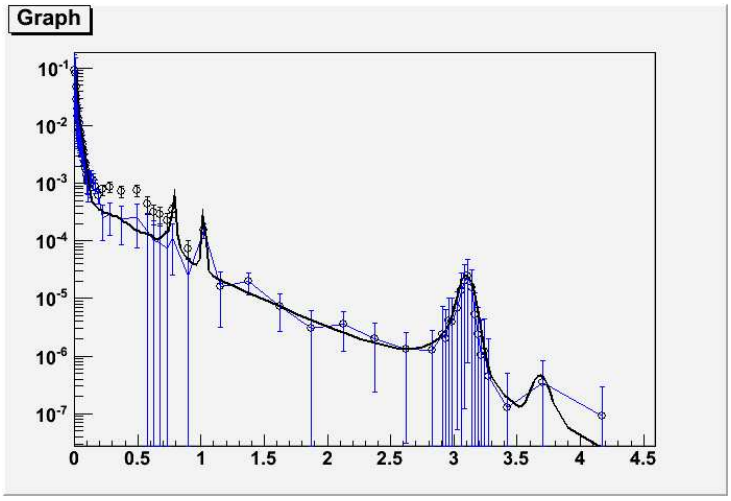

Figure 6: Projected dielectron mass spectrum for 250 million Au+Au collisions at $\sqrt{s}$=39 GeV. Black points are with low mass dielectron excess relative to the cocktail as at 200 GeV. Blue bars show the measurement and error bars if the excess is 1/3 as large. Above the ϕ meson, the blue and black are identical.

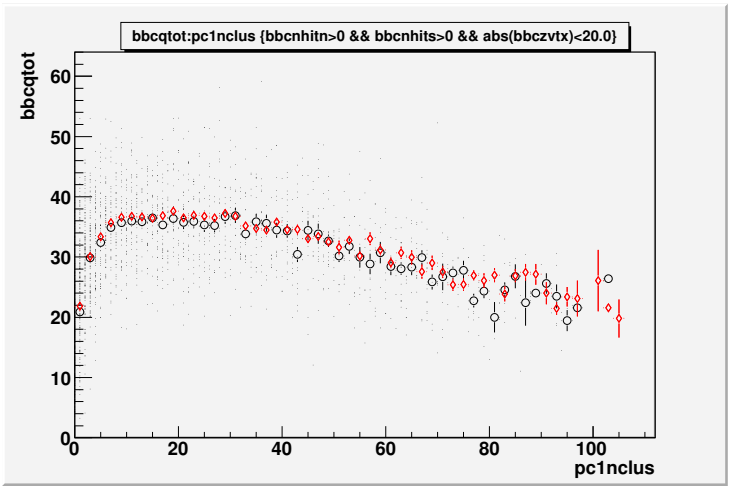

Figure 7: Total charge in the BBC vs. the number of reconstructed Pad Chamber (PC1) clusters (covering $\eta < \pm 0.35$ in 7.7 GeV Au+Au collisions. Black circles show the average of the data in each bin; red points are URQMD predictions.

parison of test data at 9 GeV Au+Au with a full detector simulation of URQMD events, indicated that with tight timing cuts the beam-beam counter coincidence provides a clean, reliable, and high efficiency trigger for very low energy collisions. URQMD was run through a fragmentation afterburner, then through a full simulation of the PHENIX detector response. The URQMD data were analyzed identically to the data, by requiring at least one hit in the north and south sides of the BBC and a reconstructed BBC z-vertex

within 30 cm of the origin. Figure 7 shows a scatter plot of the total charge in the BBC vs. the number of reconstructed PC1 clusters in 7.7 GeV Au+Au collisions. The black circles are the average of the data in each bin. The red points are from URQMD. The remarkable agreement shows that the excellent timing resolution of the BBC provides effective rejection of beam-beampipe and beam-gas collision backgrounds. Consequently, this trigger condition was used to collect 7.7 GeV Au+Au collisions in Run-10.

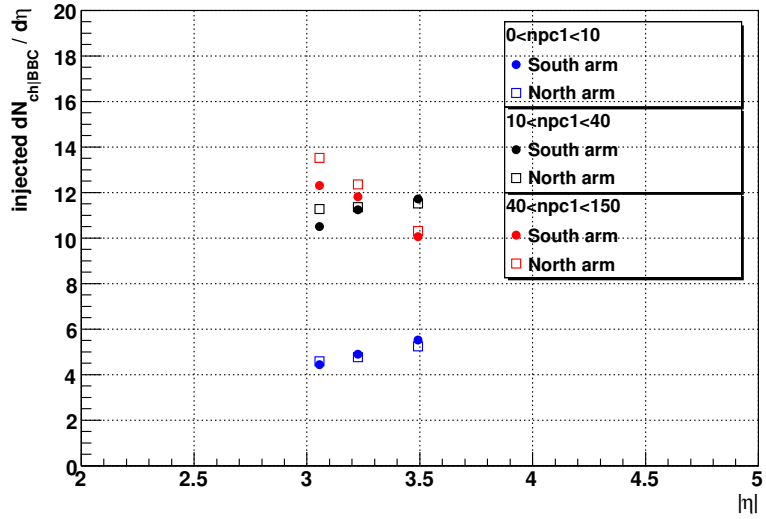

Figure 8: $dN_{ch}/d\eta$ vs. η for BBC South arm (closed points) and North arm (open squares) Three centralities are shown: central (red), semi-central (black) and peripheral (blue).

Figure 8 shows the rapidity density of charged particles measured in the north and south arms of the BBC in 7.7 GeV Au+Au collisions. In central collisions, the rapidity distribution falls with η within the BBC acceptance, while in peripheral collisions, the rapidity distribution increases with increasing η as expected for fragmentation dominated particle production into the BBC. These fragmentation products explain why the BBC trigger is efficient for peripheral collisions in addition to its efficiency for the higher multiplicity central collisions.

3.2 Recent insights from the spin program

The quark spin contribution to the proton spin has been found to be only ≈25%, indicating that the majority of the proton spin arises from the gluon contribution, ΔG, and/or from gluon and quark orbital angular momentum. PHENIX has used high energy polarized p+p collisions to access ΔG at leading order through spin-dependent gluon-gluon (gg) and quark-gluon (qg) scattering[13, 14].

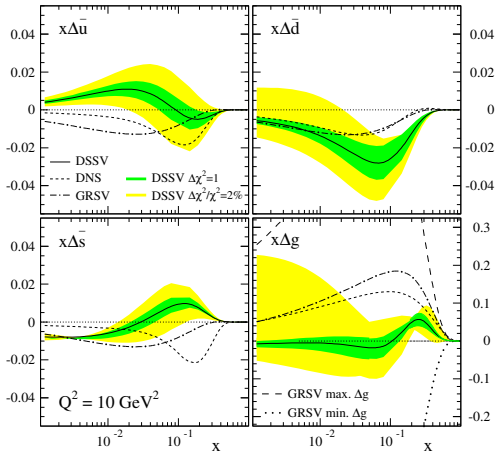

Figure 9: The polarized gluon distribution extracted from a NLO-pQCD fit[17]

The PHENIX inclusive π^0 double spin asymmetries at $\sqrt{s}$= 200 GeV, 62.4 GeV[15, 16] and the STAR jet asymmetries at $\sqrt{s}$=200 GeV form together with the world data of inclusive and semi-inclusive DIS the input to a NLO-pQCD analysis to extract the polarized quark and gluon distributions[17]. The result is shown in Figure 9. The gluon polarization ΔG = -0.084 , with a large but so far poorly determined uncertainty, for the entire x-range from 0 - 1 at Q^2 = 10 GeV^2 and ΔG = 0.006$\pm$0.06 in the x-range 0.05$< x <$0.2 covered by the RHIC data.

Figure 9 clearly shows that for $x < 0.01$ where there are no data to constrain the distribution, the uncertainties explode. Therefore it is extremely important to extend the x-range to better constrain the contribution to the integral of ΔG from low-x. This will be possible measuring double-spin asymmetries for inclusive π^0 production at 500 GeV. These measurements, combined with the existing ones at lower energy will allow meeting DOE-milestone HP12.

To ensure the measured asymmetries can be interpreted in perturbative QCD, it is extremely important to measure not only the double spin asymmetry but also the accompanying differential cross section. PHENIX has measure the unpolarized cross section for exclusive π^0 production for different center-of-mass energies (62.4 GeV, 200 GeV and 500 GeV).

3.2.1 First results from 500 GeV p+p collisions

As seen above π^0 production provides a key probe of the gluon contribution to the proton's spin. Even unpolarized π^0 measurements are of great interest, providing an important testing ground for perturbative QCD. PHENIX has measured the first π^0 spectrum in 500 GeV p+p, in order to constrain the gluon to pion fragmentation function and evaluate possible higher twist effects at high p_T. Figure 10 shows the spectrum from the Run-9 500 GeV data, compared to expectations from NLO pQCD. The agreement is very good from 2 to 30 GeV/c p_T.

W boson production has been proposed as a key probe of anti quark asymmetry [18].

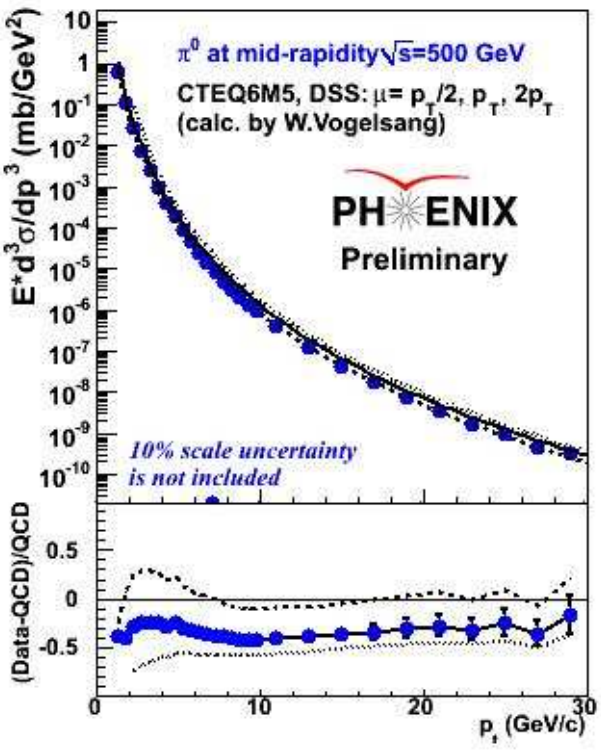

Figure 10: Invariant cross section for π^0 production in 500 GeV p+p collisions, compared with NLO predictions.

In light of the smallness of the value of ΔG observed at RHIC to date, this measurement of extreme interest. The parity violating process causes W bosons to offer a unique way to access the flavor dependence of polarized quarks in the proton. This is a complementary approach to semi-inclusive deep inelastic scattering, where the quark flavor is identified only via the fragmentation process. At leading order, positive (negative) W's are connected with u and $\bar{d}$ (d and $\bar{u}$) quarks. Furthermore, the W boson has the advantage that fragmentation functions are not needed to understand its production. In 2009, RHIC provided the first polarized proton-proton collisions at $\sqrt{s} = 500$GeV. An integrated luminosity of 8.6 pb^{-1} was sampled, with proton polarization of 35% for both beams.

In the 2009 (Run-9) measurement, PHENIX tagged W bosons by measuring decay electrons in the central arms. Figure 11 shows the transverse momentum spectrum of energy clusters in the EMCal that are associated with charged tracks of the corresponding momentum. There are components from QCD events and weak boson decays. The histogram is overlaid with curves of background and signal. The main contributions to the QCD background are charged hadron clusters and hadron decay photons which undergo conversion to electrons before the tracking system. Some are from a track mis-

association in the same jet event. The signal shape is determined by decay electrons from W and Z bosons from PYTHIA, smeared by the EMCal resolution. The dominant systematic uncertainty is from the estimation of conversion probability. There is a clear excess from W boson Jacobian peak seen in the spectra.

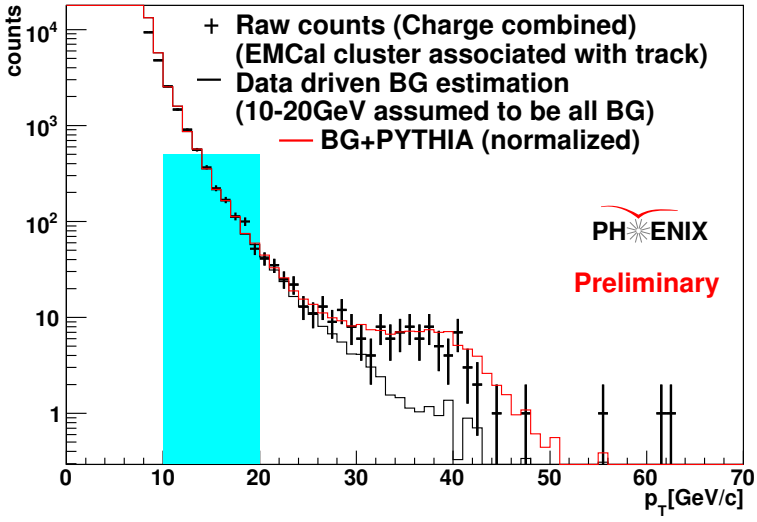

Figure 11: Transverse momentum spectra of EMCal clusters associated with a track in the PHENIX central arm detector. It is overlaid with curves of background and signal. The region of 10-20GeV is used for normalization.

For the spin asymmetry measurement, an isolation cut was applied to suppress background by a factor of ≈4. The single longitudinal spin asymmetry is defined as $A_L^W = \frac{1}{P} \cdot \frac{N^+(W)-N^-(W)}{N^+(W)-N^-(W)}$, where P is the beam polarization, and $N^{\pm}$ is the number of signal counts in positive and negative helicity beam normalized by the integrated luminosity. The sample was divided to 4 spin states (2 beams * 2 spin states), and a simultaneous fit done to extract raw asymmetries ($= P \cdot A_L$). For the physics asymmetry of W bosons, a correction for dilution by Z bosons and the QCD background is made. Figure 12 shows the resulting physics asymmetry of W^+ production. The asymmetry is consistent with predictions of various polarized PDF parametrization within 2 σ and is 2.7σ away from 0.

3.3 Recent insights in heavy ion physics

In the past year, PHENIX submitted ten papers on results from runs 4-8, and released numerous preliminary results from runs 7-9 at various conferences. We summarize here only those results directly relevant to the proposed RHIC running in 2010 and 2011. However,

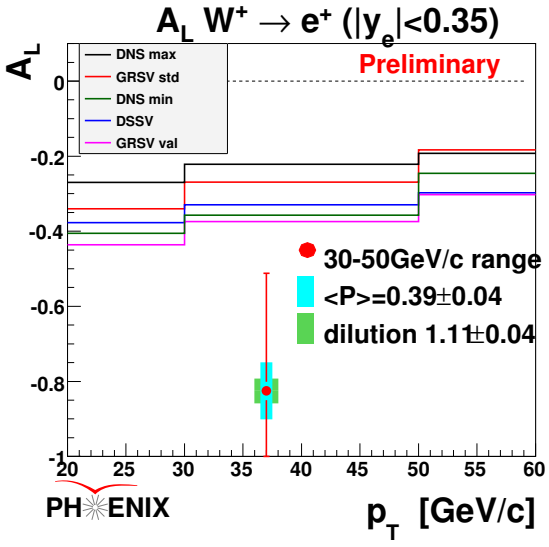

Figure 12: Longitudinal single spin asymmetry of $W^+ \to e^+$ in the mid rapidity region.

we note that PHENIX publications over the last year have reported on a wide variety of topics. These include hadron spectra, flow and suppression, jet k_T, fragmentation, and medium interactions, and charmonium polarization, in addition to dilepton production and the suppression and flow of single non-photonic electrons from heavy flavor decays.

3.3.1 Dielectron measurements

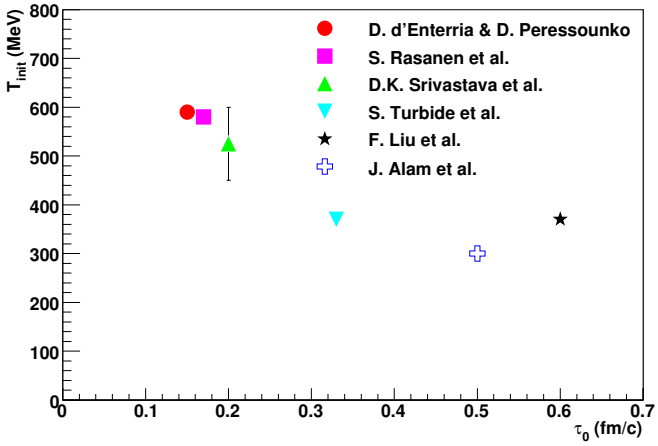

Figure 13: Initial temperature vs. thermalization time derived from a number of hydrodynamical models which reproduce the PHENIX photon spectrum. References to the models can be found in [20].

PHENIX reported first measurements of thermal photon emission, from which the initial temperature can be inferred with the aid of hydrodynamical models[19]; this temperature lies between about 300 and 600 MeV, depending on how rapidly thermalization is achieved. Strikingly, *all* of the initial temperature values lie well above the critical temperature established by lattice QCD for the phase transition to quark gluon plasma. Furthermore, the relationship between the initial temperature and the thermalization time is approximately linear with later times corresponding to lower temperature. This result, shown in Figure 13, is one of the highlights of a longer paper on dielectrons[20], received considerable attention at the Spring 2010 APS Meeting.

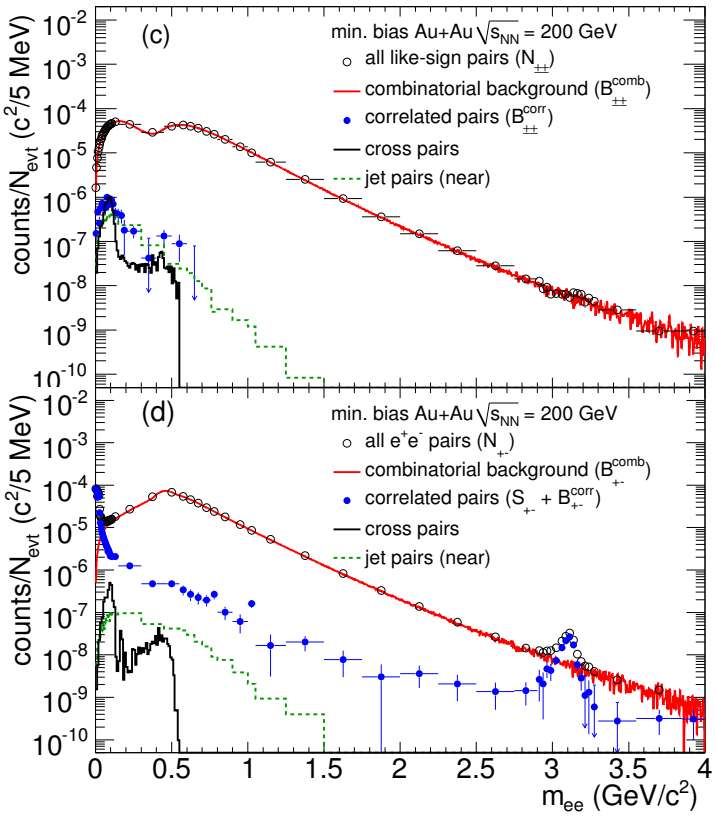

Figure 14: Dielectron spectra in Run-4 Au+Au collisions from measured and from mixed events. Top: like sign pairs. Bottom: opposite sign. Raw and subtracted spectra are shown; correlated background remaining in like sign pairs is corrected for the acceptance difference for opposite sign pairs and shown in the bottom panel.

Exhaustive analysis of the PHENIX Run-4 200 GeV Au+Au data has allowed control of the dielectron backgrounds at a level of 0.25%. Such precision is required in order to extract the true dielectron signal via subtraction; in Run-4 the signal to background at masses below 1 GeV/c^2 was $\approx$ 1:200. Figure 14 illustrates the difficulty of the problem and why substantial uncertainties from background subtraction were unavoidable in this data set. The hadron blind detector in Run-10 substantially reduces the required subtraction;

of course, data analysis is at an early stage yet, so it difficult to quantify the impact at this time.

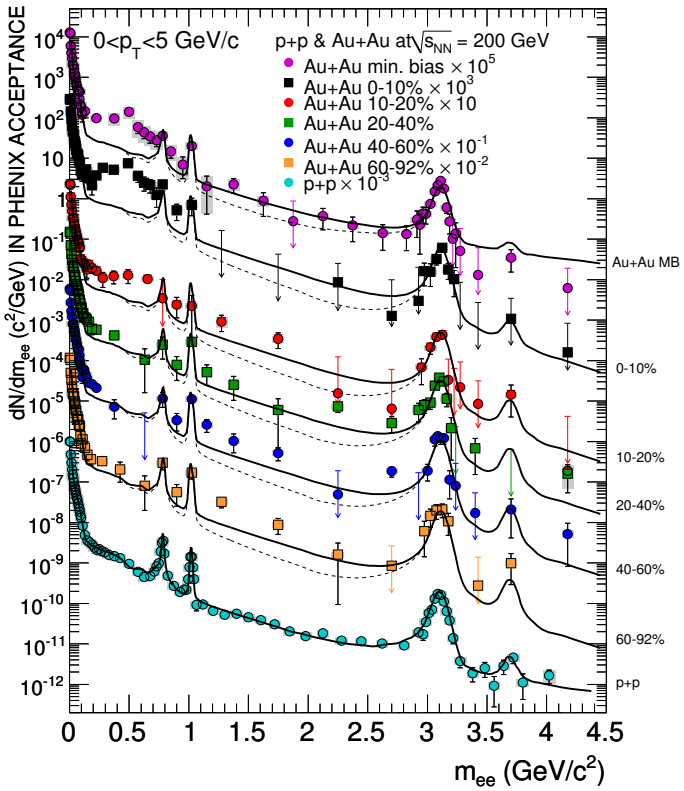

Figure 15: Invariant e^+e^- mass spectrum for different centrality classes compared to the cocktail of expected sources. Dotted lines show the expectation from uncorrelated charm decays.

After subtraction of the combinatorial and correlated backgrounds, we were able to study the centrality and p_T dependence of dielectron yields in the low and intermediate mass regions[20]. The intermediate mass region is dominated by heavy quark decays, and is discussed in the next section. Figure 15 shows a clear excess of low mass dileptons above expected sources in central collisions. Figure 16 demonstrates that this excess is concentrated primarily at low p_T, and lies substantially above all expected hadronic and partonic sources of dielectrons. The data show significant yield below mass of 400 MeV/c^2, i.e. below the region affected by in medium broadening or decreasing mass of the ρ meson [21]. Other theoretical attempts to explain this excess with combinations of hadronic collisions and quark-antiquark annihilation have been similarly unsuccessful.

The ratio $R = (data - cocktail)/f_{dir}(m_{ee})$ can be used to test whether the excess has a shape consistent with internal conversion of direct photons. Since $f_{dir}(m_{ee}$ is normalized to the data for $m_{ee} < 30$ MeV/c^2 and detector effects cancel in the ratio, R can be interpreted as the ratio of the virtual photon yield to the inclusive real photon yield. R as

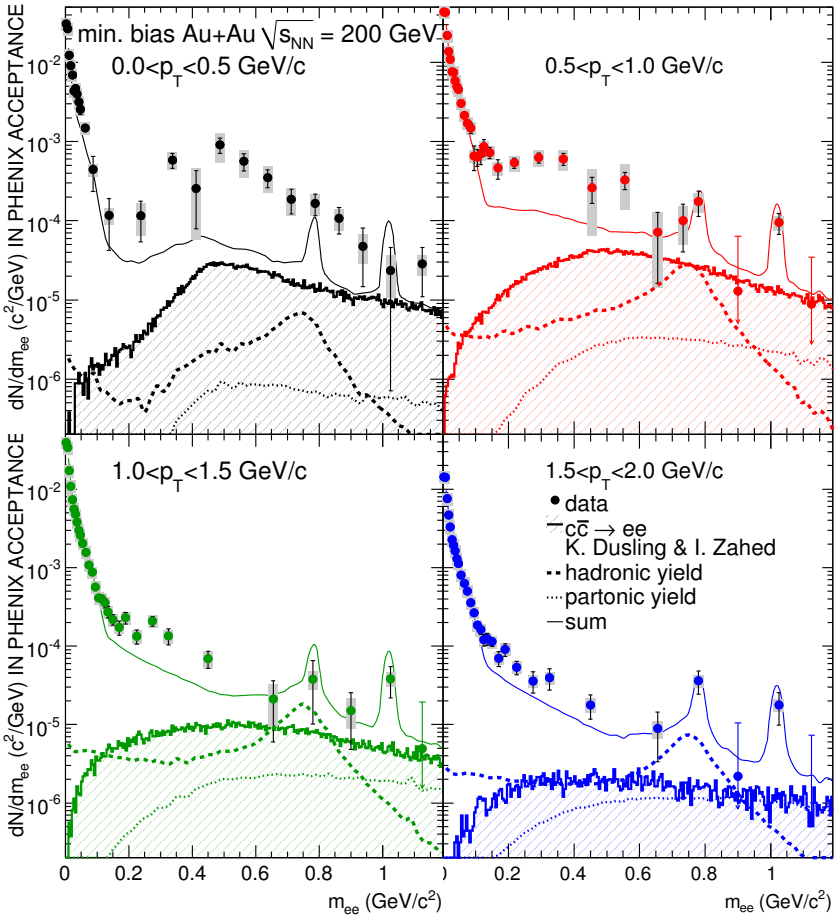

Figure 16: Invariant e^+e^- mass spectra for different p_T windows compared to calculations of Rapp and van Hees[21], separately showing the partonic and hadronic contributions and different scenarios for the ρ spectral function. HMBT indicates hadron many body theory and DM indicates dropping mass. The calculations were added to the cocktail of hadronic and charmed meson decays with the freeze-out ρ meson contribution removed.

a function of m_{ee} is shown for various p_T bins in Figure 17. On the left side are the p_T bins used for extraction of the internal conversion signal. Here the distributions are consistent with a constant, with the exception of very low mass, which suffers from substantial π^0 Dalitz decay backgrounds. Below $p_T \approx 800$ MeV/c, R begins to deviate from a constant for $0.1 < m_{ee} < 0.4$ GeV/c^2 indicating a possible additional source, though the statistical error is too large to be conclusive. We anticipate that this measurement will be much improved with the Run-10 data; initial estimates lead us to expect an order of magnitude improvement in the uncertainties at 200 GeV. The 62 GeV data set should have sensitivity comparable or somewhat better than this result. The 39 GeV data set, which was initially unanticipated, but was made possible by the superb performance of RHIC in Run-10, is sensitive to an excess larger than about 1/3 of that observed in 200 GeV collisions, as

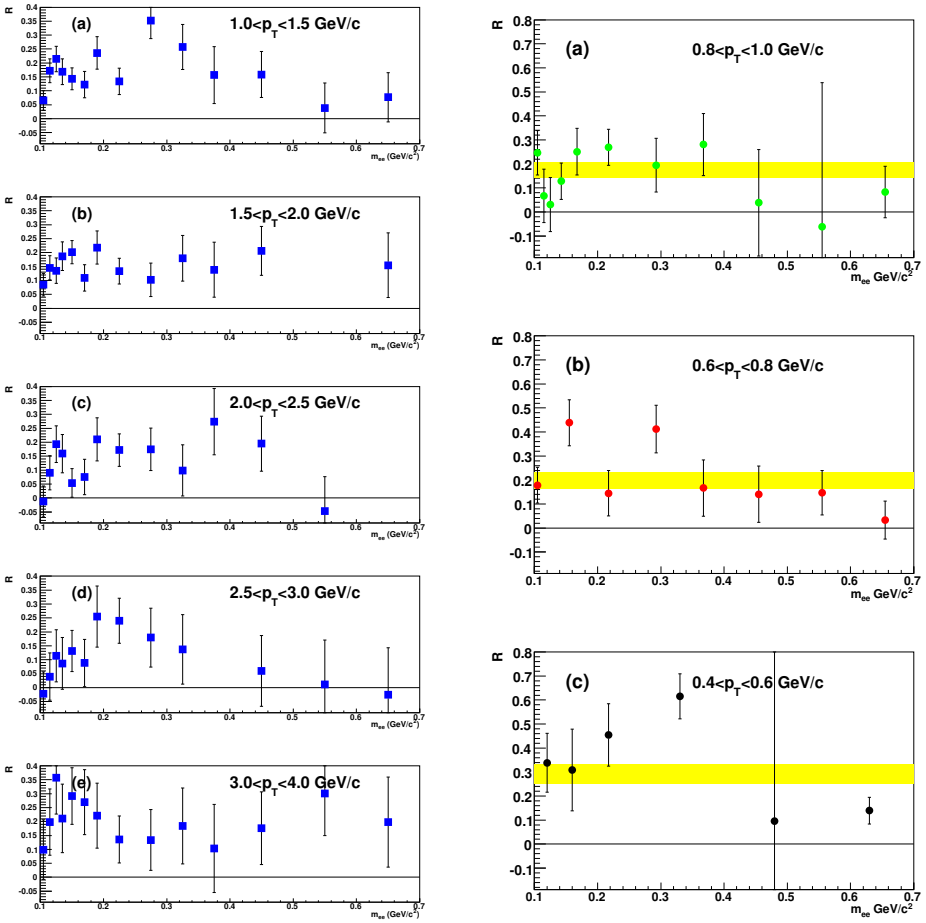

Figure 17: Ratio $R = (data - cocktail)/f_{dir}(m_{ee})$ of electron pairs for different p_T bins in minimum bias Au+Au collisions.

shown below. We anticipate analysis of the initial temperature via internal conversion of thermal photons from each of these data sets.

3.3.2 Heavy Flavor

PHENIX has shown that even charm quarks are effectively stopped by the medium: they lose a substantial fraction of the energy as they traverse the medium and participate in the collective flow along with everything else[22]. It has proven challenging to reproduce the observed light and heavy hadron suppression using perturbative descriptions of the energy loss. However, interpretation of the results thus far is complicated by the inability thus far to separate mesons containing b and c quarks in heavy ion collisions at RHIC. Addressing this need is the primary physics thrust of the PHENIX heavy ion program in Run-11 and Run-12. Key physics results, the outstanding questions, and simulated

PHENIX performance in Run-11 are detailed in section 5.3.2 below.

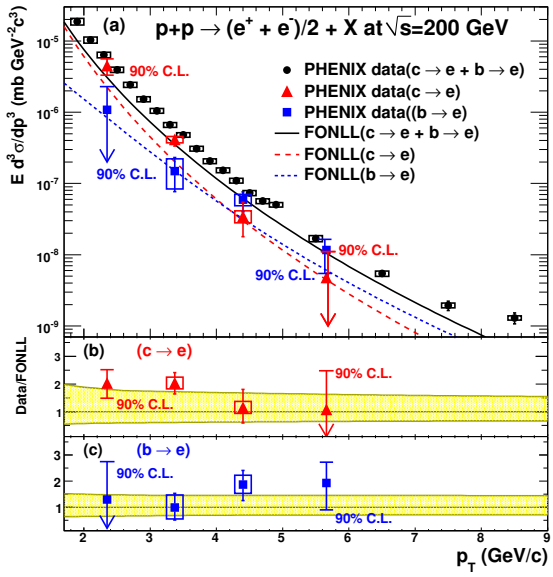

Figure 18: Non-photonic electron spectrum in p+p collisions (top); contributions from c and b decays separately are shown as triangles and squares, respectively. The comparison to FONNL predictions for heavy quarks is shown in the two bottom panels.

We have made first measurements of the c and b production cross sections separately in p+p collisions, published in Physical Review Letters[23]. Figure 18 shows the non-photonic electron spectrum in p+p collisions, and its deconvolution into single electrons from c and b decays. The deconvolution, carried out by measuring non-photonic electron-hadron correlations allowed determination of the $c\overline{c}$ and $b\overline{b}$ cross sections separately. We find $\sigma_{b\overline{b}} = 3.2^{+1.2}_{-1.1}(stat)^{+1.4}_{-1.3}(sys)\mu b$. This is consistent with our result from the dielectron spectrum[20], which gave $\sigma_{b\overline{b}} = 3.9 \pm 2.5(stat)^{+3}_{-2}(sys)\mu b$. We will utilize this result, along with high statistics non-photonic single electron spectra under analysis from the Run-8 and Run-9 200 GeV p+p data sets to provide the initial baseline for the Au+Au measurement of displaced vertex tagged electrons from c and b decays. Of course, the ultimate precision will require measurement of 200 GeV p+p collisions with the VTX detector in place; we envision requesting such a run in 2013.

4 Status of the PHENIX Experiment

PHENIX continues to utilize our high rate capability to amass large data sets. In Run-10, we recorded an unprecedented 1 petabyte data set - the first such one year volume at RHIC; for details see Table 1.

Table 2: Summary of the PHENIX data sets acquired since RHIC Run-1. All integrated luminosities listed are *recorded* values.

Run	Year	Species	$\sqrt{s_{NN}}$ (GeV)	$\int L\ dt$	N_{Tot}	p+p Equivalent	Data Size
01	2000	Au+Au	130	1 μb^{-1}	10M	0.04 pb^{-1}	3 TB
02	2001/2002	Au+Au	200	24 μb^{-1}	170M	1.0 pb^{-1}	10 TB
		p+p	200	0.15 pb^{-1}	3.7G	0.15 pb^{-1}	20 TB
03	2002/2003	d+Au	200	2.74 nb^{-1}	5.5G	1.1 pb^{-1}	46 TB
		p+p	200	0.35 pb^{-1}	6.6G	0.35 pb^{-1}	35 TB
04	2004/2004	Au+Au	200	241 μb^{-1}	1.5G	10.0 pb^{-1}	270 TB
		Au+Au	62.4	9 μb^{-1}	58M	0.36 pb^{-1}	10 TB
05	2004/2005	Cu+Cu	200	3 nb^{-1}	8.6G	11.9 pb^{-1}	173 TB
		Cu+Cu	62.4	0.19 nb^{-1}	0.4G	0.8 pb^{-1}	48 TB
		Cu+Cu	22.5	2.7 μb^{-1}	9M	0.01 pb^{-1}	1 TB
		p+p	200	3.8 pb^{-1}	85G	3.8 pb^{-1}	262 TB
06	2006	p+p	200	10.7 pb^{-1}	230G	10.7 pb^{-1}	310 TB
		p+p	62.4	0.1 pb^{-1}	28G	0.1 pb^{-1}	25 TB
07	2007	Au+Au	200	0.813 nb^{-1}	5.1G	33.7 pb^{-1}	650 TB
08	2008	d+Au	200	80 nb^{-1}	160G	32.1 pb^{-1}	437 TB
		p+p	200	5.2 pb^{-1}	115G	5.2 pb^{-1}	118 TB
09	2009	p+p	500	$\approx$ 10 pb^{-1}	308G	$\approx$10 pb^{-1}	223 TB
		p+p	200	16 pb^{-1}		16 pb^{-1}	>220 TB
10	2010	Au+Au	200	1.3 nb^{-1}	8.2G	54 pb^{-1}	885 TB
		Au+Au	62.4	0.11 nb^{-1}	700M	4.5 pb^{-1}	76 TB
		Au+Au	39	40 μb^{-1}	250M	1.6 pb^{-1}	34 TB
		Au+Au	7.7	0.26 μb^{-1}	1.6M	11 nb^{-1}	6 TB

Table 2 summarizes the data collected in Runs 1-10. For each data-set the "*proton+proton equivalent*" "*recorded*" integrated luminosity is given by the corresponding column of the table. For an A+B collision the *proton+proton equivalent* integrated luminosity is given by $\int \mathcal{L}\ dt|_{p+pequivalent} \equiv A \cdot B \int \mathcal{L}\ dt|_{A+B}$, which corresponds to the integrated parton+parton luminosity, without taking into account any nuclear enhance-

ment or suppression effects. The *recorded* integrated luminosity is the number of collisions actually examined by PHENIX, as distinguished from the larger value delivered by the RHIC accelerator. In the case of minimum bias data sets, "recorded" is strictly accurate, while for triggered data "sampled" more accurately describes the process. We use "recorded" as shorthand for either case to refer to the number of events examined by PHENIX for a given physics observable.

4.1 Future Upgrades for Installation Beyond Run-10

The PHENIX Beam Use Proposal is guided by the carefully structured, ongoing program of upgrades. Our Run-11 request is optimized to take advantage of the Muon Trigger and silicon central barrel vertex detector (VTX) upgrades. The muon trigger will allow first measurement of W production and asymmetry at forward rapidity, and the VTX will provide a first clear separation of c and b quark probes in Au+Au collisions.

The Muon Trigger upgrade construction is well underway. The front end upgrade of the muon tracker FEE is completed, with commissioning underway for Run-11 data taking. The station 3 RPCs are fully installed in the north arm and are being commissioned now. The south arm station 3 RPC's are currently being completed and will be installed in late August 2010. Final assembly of station 1 RPC's will commence in Fall 2010, and all RPC1 detectors will be installed into PHENIX in summer 2011.

The VTX assembly is currently underway and will be complete in early fall for installation prior to the beginning of Run-11. A new Be beam pipe with small diameter is nearly ready and will be installed in summer 2010. Construction of the forward vertex detector (FVTX) is well underway; the FVTX will be completed for installation prior to Run-12. Capability for forward calorimetry is needed to address key physics questions, and a conceptual design of a compact forward calorimeter optimized for d+Au physics is in internal review within the collaboration. We envision that the detector will also be utilized in Au+Au collisions to measure direct photons opposing jets detected in the VTX. Occupancy considerations will likely limit the rapidity reach of this measurement in central Au+Au collisions.

The HBD will be removed from its data-taking position (along with the RXNP) in summer 2010, in order to make room for the VTX detector.

4.1.1 Muon Trigger

Measurements of parity violating spin asymmetries in W-production with the PHENIX muon arms require a first level muon trigger that selects high momentum muons ($p >$ 10 GeV) and rejects the abundant muons from hadron decay, cosmic rays, and beam

backgrounds. The existing muon trigger identifies muon candidates based on their ability to penetrate a sandwich of steel absorber and muon detector planes. Muons with momenta above $p > 2$ GeV are selected. The resulting trigger rejection factor varies from $200 < R < 500$, depending on the (varying) beam background levels. The muon trigger upgrade introduces tracking and timing information to the muon trigger processors. The additional information will increase the muon trigger rejection by more than a factor 30.

The PHENIX muon trigger upgrade has two components: (I) new front-end electronics for the muon tracking chambers to send tracking information to new dedicated muon trigger processors. (II) Two resistive plate chamber trigger detector stations in each muon arm: RPC-1 at the entrance and and RPC-3 at the exit. The RPC stations provide both tracking and timing and are based on technology developed for the CMS muon trigger. The timing information adds background rejection power in offline analysis, particularly to remove tracks due to cosmic rays.

The baseline muon trigger upgrade for Run-11 includes the new muon tracker trigger electronics for stations 1-3 (JSPS funded) and RPC-3 installed both in the south and north muon spectrometers (NSF MRI). Also required are the first level trigger processors (LL1) that combine muon tracker hit and RPC hit information and perform the actual muon trigger alogrithm (NSF MRI).

All muon tracker trigger electronics have been installed during the summer shutdowns of 2008 and 2009 and was tested successfully during Runs 9 and 10. Complete trigger chain tests with the muon tracker trigger electronics and the LL1 trigger processors were carried out successfully during run 10. RPC-3 north was installed during October and November of 2009. The RPC production and installation remain on schedule: Figure 19 shows the alignment and pre-assembly of the RPC-3 north half octant support structures at UIUC. Figure 20 shows RPC-3 north half octants 3 and 4 during final testing in the RPC assembly laboratory at BNL, left. The right side shows the chambers being installed in PHENIX. The RPC-3 north front end electronics was installed during run 10 using accelerator access days and initial testing has been carried out. Cosmic ray system tests for RPC-3 north and the muon tracker trigger electronics are currently underway. The production of RPC-3 south is ongoing the BNL RPC detector laboratory; at the time of this report 10 half octants have been fully assembled. Assembly of the remaining 6 RPC-3 south half octants will be completed before the end of June and the high voltage burn in of RPC-3 half octants will end July 30. Installation of RPC-3 south is scheduled to begin in mid August and will be completed well before the beginning of run 11 in December 2010. RPC-1 chamber construction and installation in both arms will be completed before the start of Run-12.

Full suppression of offline backgrounds in the W-physics analysis also requires two new 35 cm thick steel absorbers upstream of the PHENIX muon spectrometer arms. 1-2% of hadrons with low momentum punch through the central magnet yoke upstream of the PHENIX muon spectrometers. A small fraction of these hadrons decays into muons in the

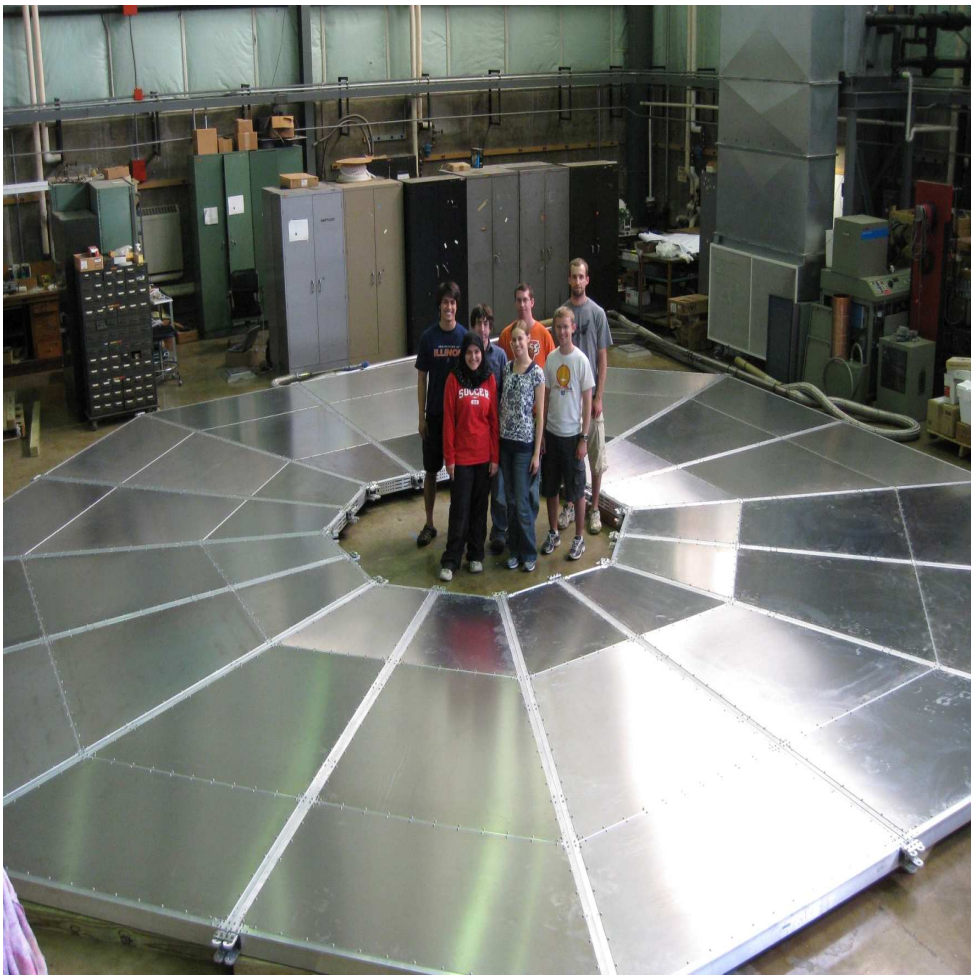

Figure 19: Pre-assembly of the RPC-3 north half octants at NPL, Urbana, together with the team.

spectrometer magnet volume such that the upstream hadron track and the downstream decay muon track overall mimic a high momentum track. We have carried out detailed Monte Carlo simulations that identify false high p_T tracks as the dominant source of the off-line background. We have shown in simulations and through data taken with a prototype absorber in run-9 that an absorber of 2 nuclear interaction lengths thickness reduces the background to acceptable levels.

The choice of absorber material is based on minimizing the additional multiple scattering from the absorber material on physics analysis and the impact the absorbers will have on the magnetic fields in the muon spectrometers. Magnetic field calculations show that SS-310 has sufficiently low permeability to keep the influence on the tracking fields negligible. The mechanical design of the absorber has been completed at BNL. The layout is shown in figure 21. Procurement of the absorber steel plates has been initiated at the University of Illinois for delivery to BNL in mid-August 2010. The two absorbers will be

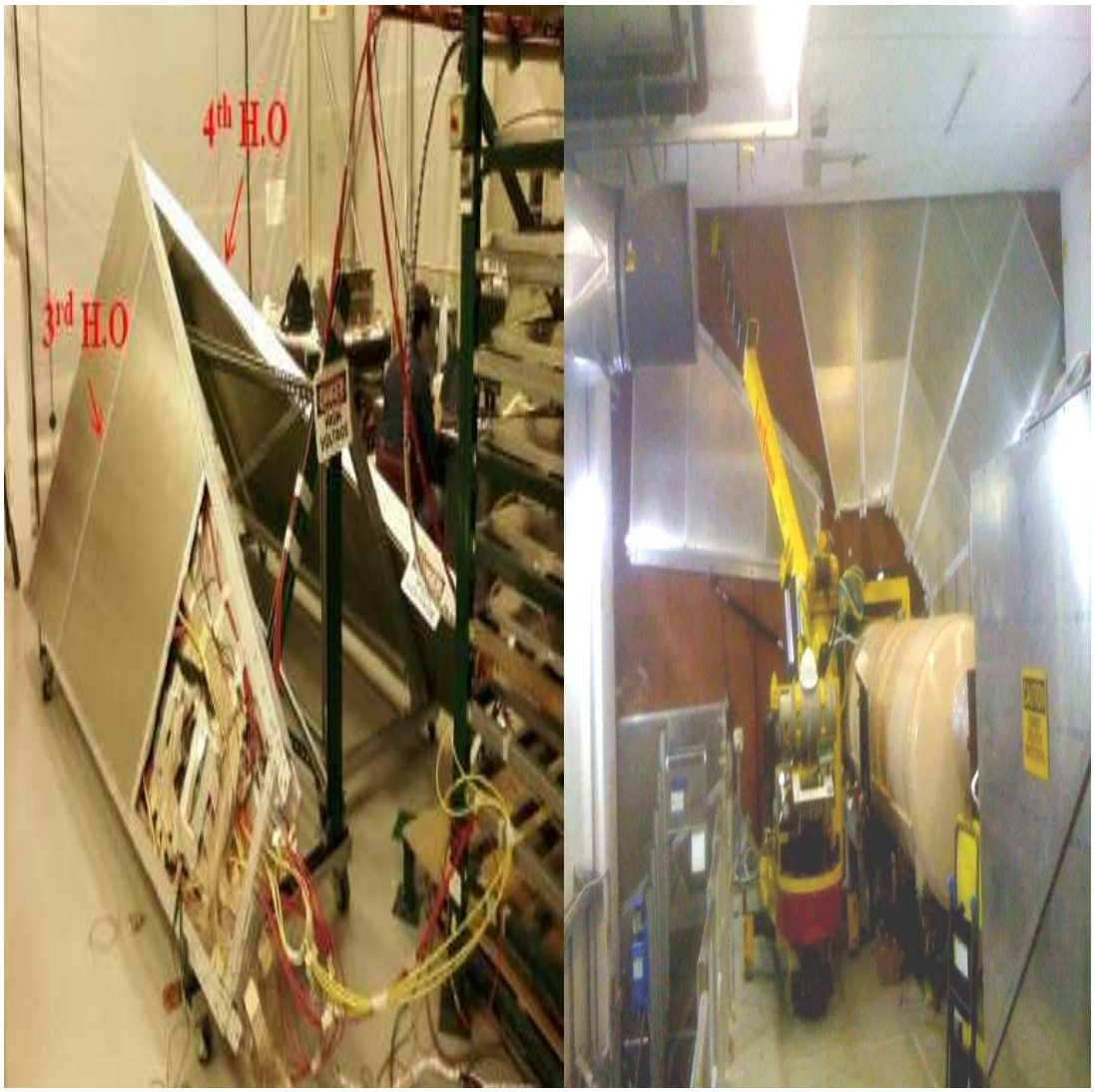

Figure 20: RPC-3 half octants being tested in RPC assembly laboratory at BNL, left and installation in progress at PHENIX, right.

installed on the south and north back faces of the central magnet yoke. The absorber installation schedule is aligned with the beryllium beam pipe installation. The beam pipe installation requires the central magnet yoke to be moved away from its regular location centered at the interaction point, resulting in straightforward access to the central magnet yoke for the absorber installation.

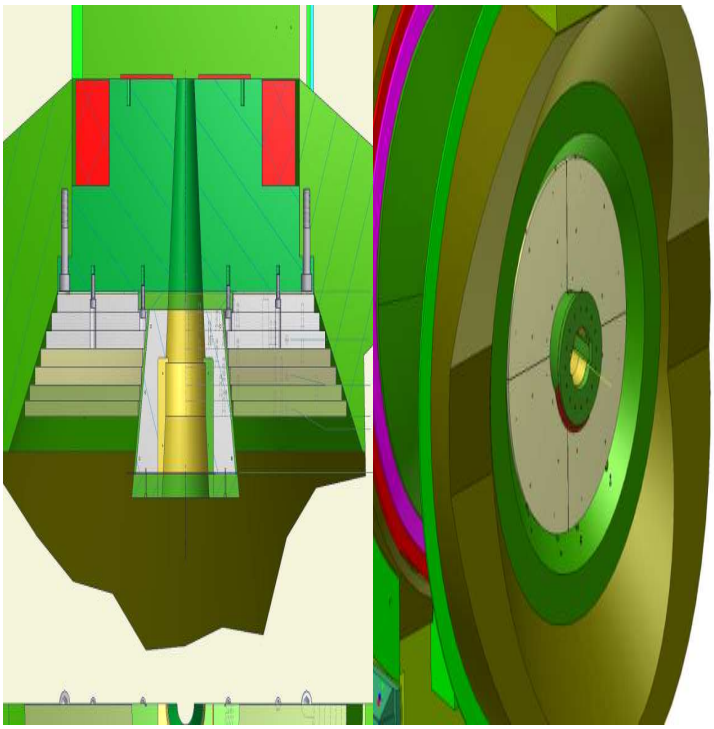

Figure 21: The muon arm steel absorbers consist of 7 rings of stainless steel plates (alloy 310). Each plate is 5 cm thick and covers one quadrant in azimuth. The absorber plates will be installed on the back faces of the central magnet yoke, upstream of the PHENIX muon spectrometers. The left plot shows a cut top view of the absorber and the right plot shows the absorber after installation of the 5th layer of steel plates.

4.1.2 VTX

Precision tracking near the interaction vertex with highly segmented silicon detectors (VTX and FVTX) is being constructed to tag products from weak decays of mesons carrying heavy quarks (charm and bottom). The primary goal is to improve the signal to background on these measurements, allow separation of charm and bottom, and provide improved mass resolution in the muon arms. The silicon detectors will be used in conjunction with the electron tracks in the central arms and muon tracks in the muon arms to measure leptons with displaced vertices from heavy meson decays. The silicon detectors also provide improved mass resolution as required to study the fate of different quarkonia in the partonic matter. The J/ψ measurements will be supplemented by ψ' and χ_C to probe the extent of color screening in the medium formed at RHIC. It should be noted that the VTX, having full azimuthal acceptance, and covering a pseudorapidity range larger than the PHENIX central arms, substantially increases the PHENIX acceptance for hadrons at midrapidity. Stand-alone tracking software performance has developed, and the VTX will greatly improve jet correlations measurements in PHENIX.

The VTX is a four layer silicon tracker at the center of PHENIX. The inner two layers pixel detectors and the outer two layers consist of novel stripixel detectors. The nominal radii of the four layers are 2.5 cm, 5 cm, 11 cm, and 16 cm, from the beam respectively. The VTX covers $|\eta| < 1$ in pseudo-rapidity and $\Delta\phi$ of 80% of 2π in azimuth. The detector can measure the vertex position of tracks with a precision of 50 μm to 100 μm, enabling identification of the decay of heavy flavors (charm and bottom). The VTX also provides large solid angle of stand-alone tracking, albeit with modest momentum resolution ($\delta p/p \simeq 5\% \oplus 10\% p$).

RUN-11 will be the first run with the VTX in place. The detector construction will be complete at the end of September, allowing installation into PHENIX prior to the beginning of the run.

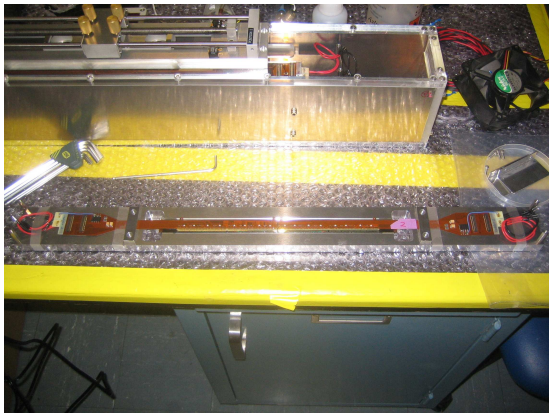

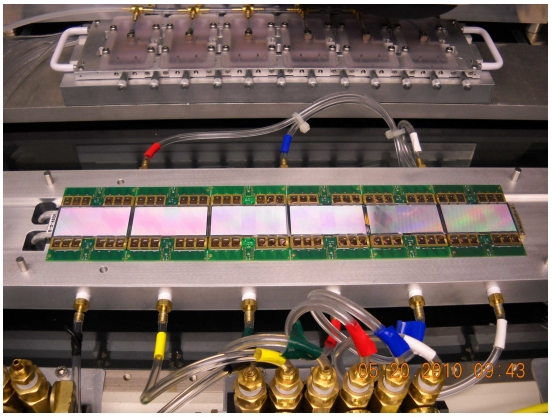

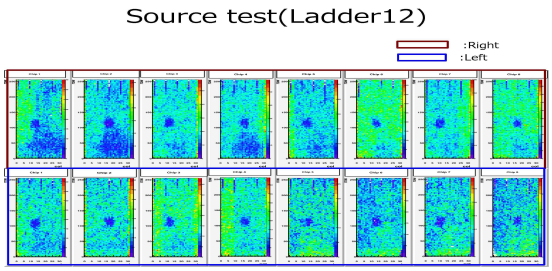

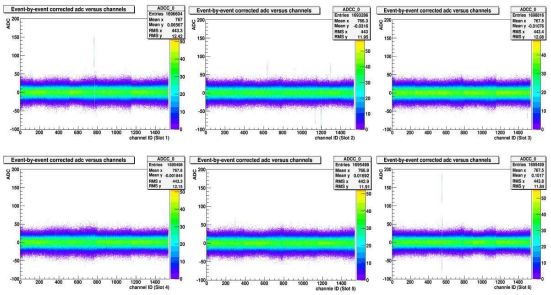

Figure 22: Top Left: Photograph of a production pixel ladder and a test bench box of a ladder. Bottom Left: Source test results of a pixel ladder. Top Right: The first production ladder of the stripixel subsystem on a stripixel ladder assembly fixture. Bottom Right: Pedestal distributions of the 6 silicon modules in the first production stripixel ladder shown above.

Pixel Detector

A pixel ladder is the basic building block of each pixel layer of the VTX. Each pixel ladder contains 4 pixel sensor modules, two high density pixel read-out buses, and a mechanical stave made of carbon fiber composite to provides mechannical support and cooling. The top left of Fig. 22 is a photograph of a production pixel ladder. The bottom left shows the results of a beta source test on a pixel ladder. The plot indicates that all 16 ALICE pixel read-out chips on this ladder work properly. The dark spot at the center of each chip is due to a small temperature sensor placed at the spot. Lower energy beta rays are stopped in the temperature sensor.

The pixel system requires 30 pixel ladders: 10 ladders for the first layer and 20 for the second layer. As of mid-May, we have assembled 15 pixel ladders at RIKEN. We project that ladder assembly will be complete in August. Assembled ladders are shipped to BNL for construction of the VTX barrel layers. The assembly of ladders into barrels will commence shortly. The left panel of Fig. 23 is a photograph of a pixel ladder test fitted on a pair of pixel barrel mounts. The barrel mounts support 5 pixel ladders, forming a half barrel of layer-1 of the VTX.

The pixel system is read-out by 60 SPIRO read-out boards. The data are then sent to PHEINX DAQ through 20 FEM boards. All of the SPIRO and FEM boards have been completed and tested.

Stripixel Detector

There are two types of ladders for the stripixel system, a longer one for layer 4 and a shorter one for layer 3. A long-type ladder has six silicon modules on a mechanical stave, while a short-type ladder has 5 silicon modules. The stripixel system needs 224 silicon modules in 24 long-type ladders and 16 short-type ladders.

We have assembled 228 silicon modules, sufficient to complete the entire stripixel system. We are currently assembling additional spare modules. Assembly of production stripixel ladders is currently underway.

The top-right of Fig. 22 is a photograph of the first production stripixel ladder being assembled on a ladder assembly fixture. Six silicon modules were glued on a carbon fiber stave under the modules and the assembled ladder was then tested. The right panel of Fig. 23 is a picture of a student working on a strip ladder prior to testing in a dark box. The bottom-right of Fig. 22 shows test results for the first production ladder. Each of the six sub-panels corresponds to one of the six silicon modules of the ladder, showing the pedestal distribution of all 1536 channels in the modules, as a 2D plot of ADC vs channel number. The plot indicates that nearly all of the 1536×6 channels in the ladder

are working properly.

The stripixel system is read-out 40 LDTB boards (one per ladder). The data from the LDTB boards are sent to PHENIX DAQ through CIB/DIB boards. Pre-production versions of these boards have been tested and worked well. Production of these downstream read-out electronics boards will commence shortly.

Mechanical System

The mechical support system consists of pixel staves, strip staves, pixel barrel mounts, strip barrel mounts, and the space frame. Fabrication of the mechanical components is either complete or nearly so at the LBNL carbon fiber composite facility. Fabrication of the pixel staves, strip staves, and pixel barrel mounts is complete. Fabrication of the space frame and strip barrel mounts will be complete soon.

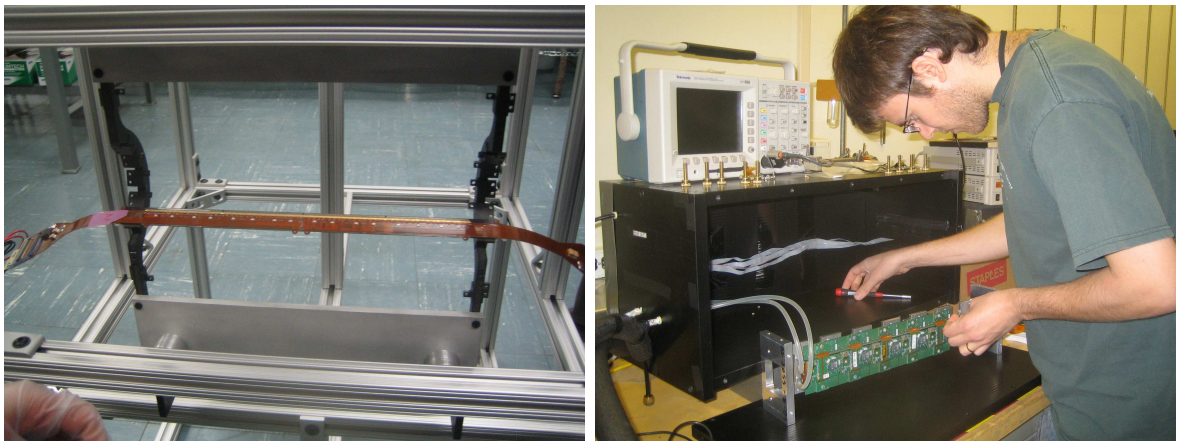

Figure 23: Left: A pixel ladder is test fitted to a pair of the 1st layer barrel mounts. Right: A student is working on a stripixel ladder before it is placed in a dark box for testing.

In summary, we are at the final construction phase of the VTX detector. Production of many of the components is complete, and the rest are nearing completion. Assembly of the detector ladders into VTX barrel layers will start soon. The construction schedule is tight but the VTX is on track to be ready for RUN-11.

4.1.3 FVTX

We are constructing two Forward Silicon Vertex Trackers (FVTX) for the PHENIX experiment to directly identify and distinguish charm and beauty decays within the acceptance

of the muon spectrometers. The FVTX will provide this essential coverage over a range of forward and backward rapidities ($1.2 < |y| < 2.4$) bringing significantly larger acceptance to the PHENIX silicon detector. This rapidity is critical for separating cold nuclear matter effects from quark gluon plasma observables. The FVTX will also substantially reduce the background and improve the mass resolution for dimuons, culminating in the first measurements of the ψ' and Drell-Yan in Au+Au at RHIC. The same heavy flavor and dimuon measurements in p+p collisions will allow us to place significant constraints on the gluon and sea quark contributions to the proton spin and to make fundamentally new tests of the Sivers function universality.

The FVTX is composed of two endcaps, with four silicon mini-strip stations in each, covering rapidity ($1.2 < |y| < 2.2$) that match the two muon arms. Each station consists of wedges of mini-strips with 75 μm pitch in the radial direction and 3.75 degree wide strips in phi, which translates to lengths in the phi direction varying from 2.8 mm at small angles to 12.1 mm at 35 degrees. An r-z DCA resolution of 100 μm can be achieved with a maximum occupancy per strip in central Au+Au collisions of less than 2.8%. A picture of the detector is shown in Figure 24 . The four stations of the North and South FVTX arms are circled in red, the central support structure for the VTX system can be seen between the two, and the large gray planes surrounding the FVTX sensors are the planes that will hold the readout electronics for the VTX and FVTX systems.

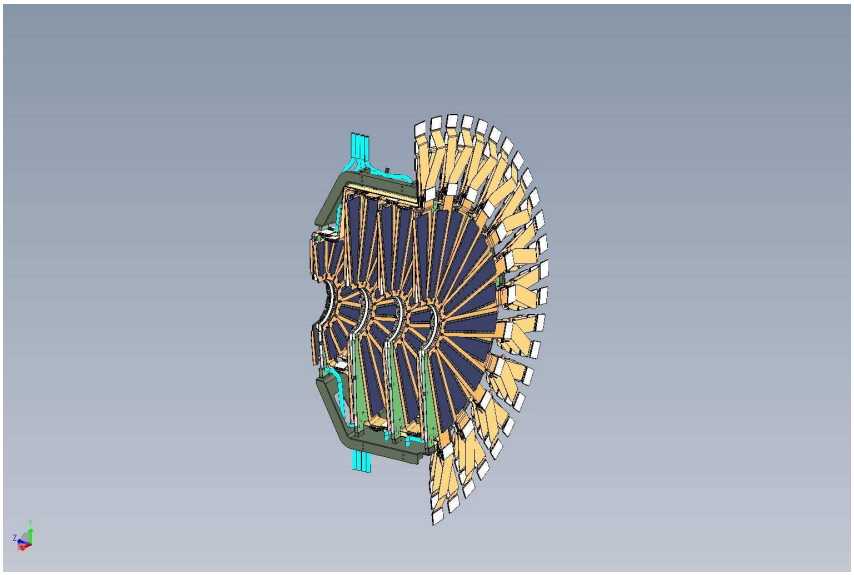

Figure 24: One half of one arm of the FVTX detector is shown, with four half-stations in view to the left of the picture and the kapton interconnect cables shown to the right of the detector. Two of these half-arms are clamshelled together around the beam pipe to form one FVTX arm.

The silicon strip sensor wedges are read out with readout chips providing analog and digital processing with zero-suppression. They produce a digital output which is "data-

pushed" at 200 Mbps to intelligent DAQ readout boards containing FPGAs. There, the data are transformed into the standard PHENIX format via two DAQ boards called the Readout Controller and the Front End Module, and transmitted to the PHENIX DAQ system via fiber optics.

An FVTX wedge "module", shown in Figure 25, is comprised of the following components: (1) a carbon fiber mechanical support structure (called the backplane), (2) a high density interconnect (HDI) kapton cable which interfaces between the silicon sensor and readout chips and our DAQ boards, (3) one silicon sensor, and (4) either 10 (for the first station) or 26 (for the other stations) readout chips which are called FPHX chips. Several FVTX prototype wedges have been assembled with all design specifications met. The production backplane support structures have all been manufactured and shipped to the FNAL SiDet facility where wedge module assembly will take place. The HDIs have been prototyped and the first batch of production HDIs have been received and shipped to SiDet for assembly of the first production modules. Approximately one half of the production sensors have been received, tested, and are ready for wedge assembly, with the final set of sensors slated to arrive in June 2010. All production FPHX readout chips have been produced, tested on the wafer, and are beginning to be diced for wedge assembly. All assembly fixtures for wedge assembly have been completed. Production wedge assembly is expected to begin the week of 1-June-2010, with all production modules assembled in approximately 7-10 months.

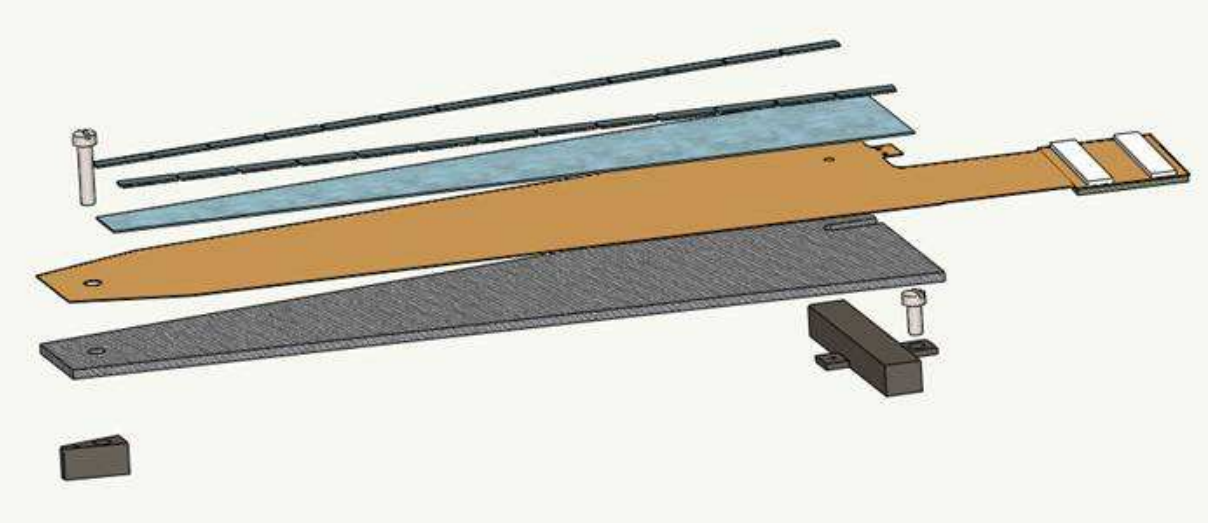

Figure 25: An exploded view of an FVTX wedge module. Two carbon fiber mounts are shown on the bottom followed by the carbon fiber backplane, the kapton HDI, the wedge sensor, and the two rows of FPHX readout chips.

The Readout Controller board (ROC) prototypes have been produced and the production design is nearing completion. All functionality of the prototype board has been verified. The Front End Module (FEM) board has also been prototyped and all func-

tionality of the prototype board verified. The final design is nearly complete and ready for production. The final DAQ board needed for the FVTX detector is a FEM Interface board which will provide an interface between the ROC and FEM boards and the PHENIX DAQ system. This board has also been prototyped and is ready for production. We expect all DAQ production boards to be ordered and received in the 2010 calendar year to allow full testing with the assembled wedge modules prior to installation in the summer of 2011.

The mechanical structures that will hold the wedge modules into station "disks" have been designed and their manufacture is slated to begin soon. The cage structures which hold 4 stations of disks to form an FVTX arm are under construction with the first production article expected in June 2010.

Production assembly of the detector will take place over the next year to prepare for installation into the PHENIX IR in the summer of 2011 with full detector testing completed by September 2011, in time for Run-12.

4.1.4 DAQ/TRIGGER upgrades for Run-11

To date, PHENIX has employed two different strategies for triggering and data acquisition for Au+Au and p+p data taking - both to great success. We have an array of fast Level-1 triggers that deliver a decision in less than 4 microseconds during which time we buffer the data from all the PHENIX detectors. In the p+p case, we have been able to successfully sample the delivered luminosity with selective Level-1 trigger based on identified muons at forward rapidity and photons and electrons at mid-rapidity. In Au+Au collisions many key topics do not have the possibility of selective Level-1 triggers (for example low mass dileptons or low to modest p_T electrons from heavy flavor; the latter is the focus in the upcoming 200 GeV Au+Au run). In Run-10, improvements in the timing system firmware, custom data collection module (DCM) software and data compression, along with noise reduction in outlying front end electronics allowed the PHENIX data acquisition to sustain an archiving rate of 5000 Hz. In fact, we recorded in full 8.2 billion minimum bias Au+Au events at 200 GeV $\sqrt{s}$ (1.3 inverse nanobarns) in Run-10, corresponding to 76.5% of all interactions within $|zvertex|$ <30 cm (i.e. in the acceptance of the PHENIX central arms). We also ran the electron/photon Level-1 trigger during the second half of the run, however it sampled only a modest additional luminosity since we recorded the bulk of all interactions.

In the projected full energy Au+Au in Run-11, CAD projects a modest delivered luminosity increase, but the effective acceptance of the PHENIX central arm spectrometer with the VTX detector is reduced to interactions within $|zvertex| < 10$ cm. Thus, for the upcoming run the strategy of recording the bulk of minimum bias events is the most effective and efficient. In Run-11, the VTX is estimated to increase the total data volume

by a factor of 1.5 (in Run-12 adding the forward vertex detector FVTX increases this factor to 1.7). Consequently, to maintain 5 kHz bandwidth, PHENIX requires a 50% increase in total Megabytes/seconds archiving rate as well as new readout electronics and data acquisition components. A new generation of Data Collection Module II based on the Altera STRATIX FPGA core has been designed to allow this. DCM II modules are in production for receiving the data from the new detectors with a full rate specification of 8-10 kHz, even for the event sizes of full energy Au+Au collisions.

The data are transferred at 10 Gigabit/second rates to a custom PCI express board (referred to as the JSEB II) which resides in a new set of Sub Event Buffer (SEB) machines. These machines have a 10 Gigabit/second network card and will interface with a new switch, which has been ordered (a Force10 with 2x96 Gigabit ports and 20 10GbE ports). All ports are non-blocking; any 2 can sustain the respective max throughput between them concurrently. We will add Bufferboxes according to need. The current plan is to buy more Gig-based ones (since each 10GbE port costs about 3000 dollars, it is more economical to add more machines rather than take the existing ones to 10GbE). From the HPSS/RCF point of view, we already clarified that this is feasible on a schedule commensurate with installation of the new detectors. By driving the existing Bufferboxes harder and supplementing their number, we will be able to at least double the capacity. In Run-10 PHENIX approaches a network bandwidth limit only at the very beginning of a fill (in full energy Au+Au collisions). The components described above comprise the PHENIX DAQTRIG2010 upgrade.

As the new VTX detetor and new data acquisition components will be commissioned in Run-11, we have conservatively estimated a DAQ bandwidth performance of 2.5 kHz for 200 GeV Au+Au collisions. The specifications for the new VTX readout and DAQ should ultimately allow a 8-10 kHz performance, and thus we would be limited at 5 kHz by the existing detector system readout. We hope to achieve the 5 kHz rate by the end of the Au+Au running period.

An additional factor in data taking efficiency is that after beam injection and cogging, PHENIX has required re-synchronizing our front end electronics to the RHIC clock based on the beam cycle itself. During the 7.7 GeV Au+Au part of Run-10, we were able to devise a system with a sufficiently stable clock transition to remain locked for all fiber connections and FPGAs, avoiding this re-synch. This was crucial for data taking at low energy due to the very short store time (as low as 10 minutes). This improvement will also improve our uptime for the other colliding systems and energies. We still require the ramp down of some high voltages during beam injection and steering, however we will begin physics sampling more reliably by avoiding the occasional synchronization failures inherent in switching clocks at each store.

4.1.5 FOCAL

In order to pursue several critical physics measurements in both spin and heavy ion physics, PHENIX requires coverage for photons, π^0's and jets at forward rapidity. This will dramatically increase the acceptance for direct photons, photon+jet or two π^0s in the final state. In p+p and d+Au direct photons probe the parton distribution function with added sensitivity, and correlations constrain the kinematics of the hard collision by measuring $x_{Bjorken}$. In d+Au collisions PHENIX will be able to probe the nuclear gluon distributions to lower x, which is critical to pin down the initial conditions in heavy ion collisions, and is of prime interest in its own right. Shadowing and gluon saturation in heavy nuclei are under intense theoretical discussion, and require high quality new data.

PHENIX has developed a design for a FOrward CALorimeter (FOCAL), which is a novel, compact calorimeter composed of tungsten absorber with silicon pad readout. A coverage of approximately $1< |\eta| <3$ and 2π in azimuth in envisioned, with a depth of 24 X_0. The location of FOCAL is on the front of the PHENIX muon magnets. The readout of the pads in several layers allows the longitudinal as well as lateral profile of showers to be used to reject hadronic background. In order separate photons and π^0's, layers of high resolution silicon strip detectors are inserted within the first several radiation lengths. FOCAL will be able to reconstruct the π^0 invariant mass to an energy of about 60 GeV. The FOCAL design has been extensively simulated, an early prototype was tested with beam in summer 2009. A detailed proposal and cost estimate are currently in internal review by the PHENIX Collaboration.

5 Beam Use Proposal for Run-11 and Run-12

5.1 Planning Assumptions and Methodology

The Associate Laboratory Director for Nuclear and High Energy Physics has directed the experiments to plan assuming 25 or 30 weeks of cryo operations in Run-11 and 25 cryo weeks in Run-12.

Detailed guidance provided by the Collider-Accelerator Department (C-A D) describes the projected year-by-year luminosities for various species, along with the expected time-development of luminosity in a given running period[24]. We have used the species-dependent luminosity guidance, the stated cool-down time, and the stated start-up and ramp-up time for each species to convert the required delivered integrated luminosities into a plan for the approximate number of weeks at each species. We also take into account an additional week of set-up to develop polarization in 500 GeV p+p collisions. Based upon the by-now extensive experience with operating RHIC in a variety of modes, we use

the geometric mean between the projected minimum and maximum delivered luminosity. We applaud C-A D developments of stochastic cooling, and request annual full energy Au+Au runs to utilize this key improvement in RHIC capabilities for physics production. We understand that not all of the stochastic cooling cavities may be available in Run-11, however a first look at the exciting new physics with the PHENIX VTX does not require the highest possible luminosity for the inaugural run. As the EBIS source will become available in 2011, we look forward to a program utilizing collisions of U+U, beginning with a short run at initially low luminosity to enable us to calibrate the selection of different asymmetric collision geometries of these significantly non-spherical nuclei.

Based on the CA-D guidance [24], we assume the following for luminosities and polarization (please see below for explanation of the difference between delivered and recorded or sampled luminosity):

- Based upon 500 GeV p+p in Run-9, we assume that a goal of 150 pb^{-1} delivered can be reached in 10 weeks. This represents only a small increase over the instantaneous luminosity observed during the last 3 weeks of the 500 GeV run. The integral is attainable with 10 successful stores per week.
- Our plan for 500 GeV p+p running utilizes the projected polarization of 50% in Run-11. Should this not be attained after 4-5 weeks of physics running, we anticipate that the goals and run length in Run-11 may be re-optimized. Our total goals are to sample $50 pb^{-1}$ in Run-11 and 100 pb^{-1} in Run-12.
- After the ramp-up period, average Au+Au delivered luminosity per week at $\sqrt{s_{NN}}$ =200 GeV is 775 $\mu\mathrm{b}^{-1}$ in Run-11 and 990 $\mu\mathrm{b}^{-1}$ in Run-12.

In order to determine the fraction of delivered luminosity that can be recorded by PHENIX, we utilize the following factors:

- The PHENIX live-time is taken as 97%, which is the same as that in Run-10. We anticipate maintaining this factor also in p+p by avoiding the point where the DAQ bandwidth saturates.
- The PHENIX uptime is taken to be 65%, commensurate with recent data taking with full energy Au+Au.
- We assume that there will be some success with implementing the 9 MHz cavity to reduce the longitudinal emittance in proton beams. Consequently, our planning reflects 20% of the p+p collisions inside $\pm$10 cm and 55% inside $\pm$30 cm.
- 25% of Au+Au collisions at $\sqrt{s}$ 200 GeV/A are assumed to be inside $\pm$10cm. This is the value projected by CA-D for Run-11, and is slightly smaller than the value measured in PHENIX during Run-10.

For most of the polarized p+p and full energy Au+Au running, the projected collision rates are sufficient to reach the PHENIX bandwidth limit. Consequently, we will trigger primarily on rare processes in p+p (e.g. high momentum leptons and photons) and implement several vertex cuts at the trigger level for Au+Au data taking. The physics performance studies presented below for these two species for Run-11 have been done under the following assumptions:

150 pb−1 delivered integrated luminosity in 10 weeks of physics data taking for 500 GeV p+p. This yields 50 pb^{-1} sampled inside a vertex of ± 30 cm for the W measurements in the muon arms via

$$(\mathrm{PHENIXlive} = 0.97) \times (\mathrm{PHENIXup} = 0.65) \times (\mathrm{vertex} = 0.55) = 0.35\%$$

It may be found that events outside a 30 cm vertex cut can be successfully utilized. However until that is demonstrated with data, we plan the running time assuming a 30 cm vertex cut.

In full energy Au+Au we assume data taking at an average data acquisition rate of 2.5 kHz, though we anticipate that the maximum possible data taking rate will be nearer to 5 kHz.

- Initial physics running at luminosities that do not yet saturate the PHENIX DAQ bandwidth.
- Time for commissioning of new DAQ elements.
- Possibility of increased data size due to detector noise on the maiden voyage of the VTX.

We also assumed a PHENIX uptime of 65% and a RHIC uptime of 60%. We note that in the newest projections, the RHIC uptime is projected to be 55% instead. However, the difference of 5% is well inside the uncertainty of our estimation procedure. Furthermore, it is likely to cancel with improvements in PHENIX data taking efficiency achieved via repairing the technique for locking the PHENIX clock to the RHIC clock.

To estimate luminosity and vertex cut effects for low energy p+p collisions, we utilize Figure 2 in the CA-D projection document[24] for the bunch length scaling, along with projections for the lowest energies from Wolfram Fischer (private communication).

5.2 Beam Use Proposal Summary

This proposal is designed to maintain the program of discovery physics that has attracted world-wide attention to the RHIC heavy ion program, *while maintaining* progress in spin

physics to continue the search for the carriers of the proton's spin. In parallel, PHENIX is constructing key detector upgrades. These continually enhance our capabilities and open new avenues to pursue compelling physics questions that were unknown at the dawn of the RHIC. This beam use proposal is crafted to utilize the new capabilities as soon as they become available. The PHENIX philosophy is accomplished by

- Optimizing the RHIC run plan to take advantage of key detector upgrades as they become available.
- Targeting physics goals to utilize RHIC luminosity and ion source improvements in both the heavy ion and spin programs. This consideration is also critical running below injection energy.
- *Completing* surveys by securing requisite baseline data in a timely fashion, so that comparison data sets are obtained with essentially the same detector configuration.
- Continued enrichment of existing data sets that are statistically sparse in essential physics channels (which requires accumulation of data over multi-year periods)

Table 3: The PHENIX Beam Use Proposal for Runs 11-12.

RUN	**SPECIES**	$\sqrt{s_{NN}}$ **(GeV)**	**PHYSICS WEEKS**	$\int \mathcal{L}dt$ **(recorded)**	**p+p Equivalent**	**Polarization**
11	p+p	500	10	50 pb^{-1}	50 pb^{-1}	50%
	Au+Au	200	8	0.7 nb^{-1}	28 pb^{-1}	
	Au+Au	27	1	35M events		
	Au+Au	18	1.5	37M events		
	U+U	192.8	1.5	150-200M events		
12	p+p	500	8	100 pb^{-1}	100 pb^{-1}	50%
	Au+Au	200	7	0.7-0.9 nb^{-1}	28-36 pb^{-1}	
	p+p	62.4, 22.4	2.5	1.0, 0.01 pb^{-1}		0%

The highest priority for PHENIX is to utilize the new Muon Trigger upgrade for first measurement of W asymmetry at forward rapidity and to utilize the new silicon vertex detectors to separate charm and bottom to investigate the mass dependence of energy loss by heavy quarks in quark gluon plasma. These goals necessitate running 500 p+p with good polarization in both 2011 and 2012, and running full energy Au+Au collisions in both years.

Our next priority is to fully exploit the energy scan data collected in Run-10. This necessitates collecting reference p+p data at several low energies, and collecting a substantial set of data with Au+Au collisions at $\sqrt{s}$ of 27 and 18 GeV.

We anticipate beginning the study of U+U collisions during this running period. It is the judgment of the PHENIX collaboration that this study is best accomplished with two separate runs. An initial small U+U data set will be collected as part of commissioning of uranium beams in the new EBIS source. This will allow development of methods to control/select the geometry of collisions in this non-spherical system, event by event. Armed with the results of this study, an optimum set of target observables can be determined, and the required running time evaluated.

The ALD has charged the program to propose a run plan for 25 cryo weeks in Run-11, in case budget pressures in FY11 dictate a shortened running. PHENIX proposes modifying the above plan with the steps enumerated below; time modification to the running schedule proposed in Table 3 are listed in the order PHENIX prefers (i.e. in inverse order of priority for data taking).

- Shorten U+U from 1.5 weeks to 0.5 weeks
- Shorten 500 GeV p+p from 10 weeks to 8.5 weeks
- Remove Au+Au at 18 GeV.
- Shorten 200 GeV Au+Au from 8 weeks to 7 weeks.

5.3 Run-11

The twin top priorities for PHENIX in Run-11 are polarized proton running to make progress toward our spin physics goals, and full energy Au+Au running to utilize the new VTX detector for a first separation of charm and bottom in heavy ion collisions.

It is the conclusion of the collaboration that until the p+p luminosity is increased by implementation of electron lenses, it is more productive to run polarized proton collisions at 500 GeV than to enlarge the data set at 200 GeV. The smallness of both ΔG and the achieved and projected luminosities mean that a significant improvement upon the 200 GeV Run-9 data set is difficult in the short run. On the other hand, Run-11 will see the majority of the muon trigger upgrade installed. PHENIX will have in place all Muon tracker FEE components, and RPC3's in both arms. Furthermore, a layer of additional shielding will be installed at the front face of the muon arms. This leaves us with full functionality for the online W trigger. The RPC1's, to be installed in the shutdown following Run-11, provide additional timing information and improve the offline background rejection, particularly of cosmics. However, even without this, a first W asymmetry physics run is feasible with good performance. Consequently, PHENIX requests 50 pb^{-1} sampled (150 pb^{-1} delivered) of 500 GeV polarized proton collisions. The required polarization is 50%. We estimate that 9.5-10 weeks of physics running will be required to reach this goal.

The physics delivered with this first 500 GeV production run is two-fold, as described in detail below. We will make first W asymmetry measurements to look at light quark and anti-quark polarization. And, we will measure ΔG via midrapidity π^0 A_{LL}. The two lowest x points at 500 GeV fall below the lowest x points in the 200 GeV data, extending our sensitivity down to $x < 0.02$.

In parallel with key spin physics measurements, this run will allow commissioning of the PHENIX central barrel silicon vertex detector (VTX). As described above, construction is nearly complete at this time, and the detector will be installed for Run-11. Our plan allows for commissioning of the VTX with p+p collisions, followed by physics running to yield a first measurement of separated open charm and bottom energy loss and flow with VTX.

Our next priority is to fully exploit the energy scan data collected in Run-10. This necessitates collecting reference p+p data at several low energies, and collecting a substantial set of data with Au+Au collisions at $\sqrt{s_{NN}}$ of 27 and 18 GeV. In order to fully utilize the energy scan data collected at 62 and 39 GeV in Run-10, we request p+p collisions for comparison at the same energies. A data set at 22.4 GeV is particularly important, as it will provide baseline data to pin down the pion R_{AA} in Cu+Cu collisions. This measurement would also allow the intermediate energy p+p yields to be interpolated instead of extrapolated, providing an improvement in the excitation function of energy loss until the full comparison data sets are available.

We anticipate beginning the study of U+U collisions during this running period. We request an initial small U+U data set in Run-11, to be collected as part of commissioning of uranium beams in the new EBIS source. This will allow development of methods to control/select the geometry of collisions in this non-spherical system, event by event. As this utilizes observables with large cross section, a small number of events will suffice for this study.

5.3.1 Polarized proton running at 500 GeV

The highest priority for PHENIX Spin for Runs 11 and 12 is the 500 GeV longitudinal spin program described in [14]. This plan requires sampling 150 pb^{-1} at PHENIX, which implies the delivery of approximately 450 pb^{-1} to our interaction point. These data will enable us not only to make significant measurements of the gluon spin polarization in the proton, using a variety of probes, but also to measure single-spin asymmetries in W production leading to the measurement of the light anti-quark spin polarizations.

Through Run-9, PHENIX has recorded a total of approximately 25-30 pb^{-1} (summed over Runs 5, 6, and 9) of polarized pp collisions at 200 GeV. Our goal at 200 GeV had been to record approximately 70 pb^{-1}, however it is clear that with currently achievable

luminosity meeting this goal would require several more years. The double spin asymmetry in inclusive π^0 production, $A_{LL}^{\pi^0}$, is consistent with zero in the transverse momentum range $1 < p_T < 10$ GeV/c, limiting the gluon spin contribution to the proton spin in the parton momentum range $0.02 < x_g < 0.3$ to $-0.7 < \Delta G^{[0.02,0.3]} < 0.5$ at 3σ[15]. Consequently, it is best to move forward with accumulation of statistics at 500 GeV, to extend the study of gluon polarization to smaller x_g and begin exploration of the spin polarization of $\bar{u}$, and $\bar{d}$ quarks via the parity-violating asymmetry in and W boson production. Furthermore, the higher luminosity of collisions at 500 GeV compared to 200 GeV will finally put measurement of the direct photon asymmetry within reach, opening an independent determination of ΔG. In direct photon production the gluon Compton process ($qg \rightarrow q\gamma$) is dominant, so the double helicity asymmetry will be linear with gluon polarization. Consequently, PHENIX will be able to measure both the sign and value of ΔG through this channel.

It is imperative to collect sufficient data before 2013 to achieve NSAC milestone HP8, which requires measurement of flavor-identified q and $\bar{q}$ contributions to the spin of the proton via the longitudinal-spin asymmetry of W production in calendar year 2013. We anticipate that this milestone can probably be at least partially satisfied with with the requested luminosity, the ultimate result will require 900 pb^{-1} delivered luminosity. In Runs 11-14, the beam polarizations should be at least 50%, and increase to 60% as soon as possible.

The parity-violating asymmetry $A_L^{W^\pm}$ in the production of $W^\pm$ bosons permits the determination of the light-quark and -antiquark polarizations in the proton. In PHENIX this will be done via the detection of high p_T electrons/positrons in the central arms from the decay $W^\pm \rightarrow e^\pm\nu$ and of high p_T muons in the muon arms from $W^\pm \rightarrow \mu^\pm\nu$. Our simultaneous coverage in forward, backward, and central rapidity will provide a powerful means of determining the quantities $\Delta\bar{u}/\bar{u}$, and $\Delta\bar{d}/\bar{d}$ in the parton momentum range $0.05 < x_{Bj} < 0.6$. Almost direct quark/anti-quark separation is possible with forward/backward leptons from W- production in the PHENIX muon arms due to much larger quark density vs anti-quark density at large momentum transfer. In this case, $A_L(\text{forward } W^- \rightarrow \mu^-) \approx \Delta d/d$. Similarly, $A_L(\text{backward } W^- \rightarrow \mu^-) \approx \Delta\bar{u}/\bar{u}$. Additionally, measurement of W^+ production will give access to $\Delta u/u$ and $\Delta\bar{d}/\bar{d}$. However, due to the fixed neutrino helicity, the flavor contributions in forward and backward rapidity are mixed. Similarly, the parity-violating asymmetry of W^+ production in central rapidity combines contributions from both u and $\bar{d}$ polarizations, and from d and $\bar{u}$ polarizations in W^- production. These measurements will have their greatest impact in improving global fits that seek to determine the polarized parton distribution functions in the proton.

Figure 26 shows our expectations, assuming 50% polarization, for the asymmetry uncertainties with 50 pb^{-1} sampled in the muon channel. The curves show the results of various pQCD fits including different inclusive and semi-inclusive DIS data along with RHIC polarized p+p data from previous runs. The left side shows the expected error bars

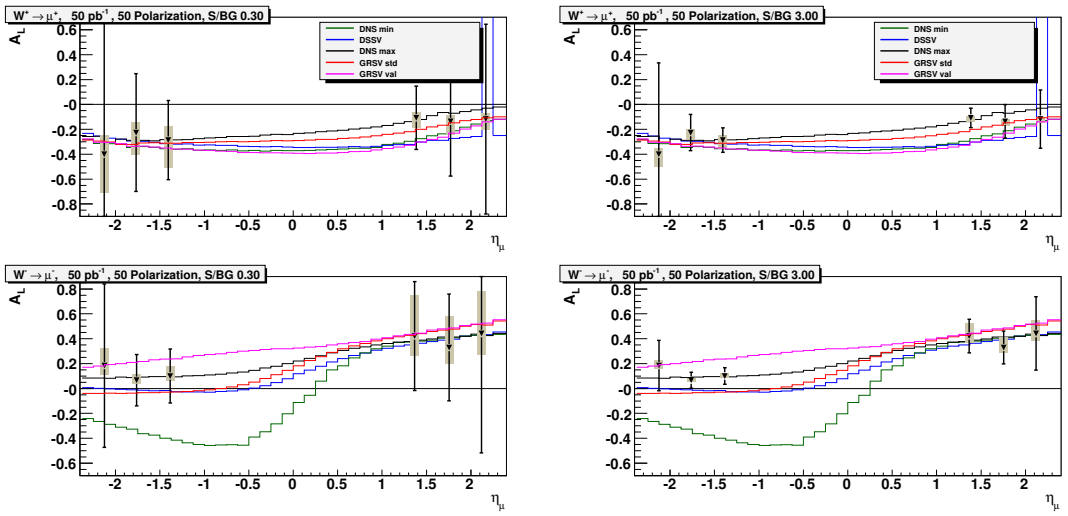

Figure 26: Expectation for uncertainties in W asymmetry measurements with 50 pb^{-1} recorded with 50% polarization. Left side shows the projected uncertainties with S/B=0.3 and the right side with S/B=3.0.

from Run-11 for S/B = 0.3, which is a very conservative estimate once the absorber is installed. The right side shows the result with S/B = 3.0, which we hope to be able to achieve.

Combining Run-11 and Run-12 500 GeV p+p runs, will provide 150 pb^{-1}. Should the background rejection prove difficult to achieve with offline cuts and the absorber, the FVTX can be used for further rejection power beginning in Run-12. In this case, a tighter vertex cut will be required, resulting in approximately 50 pb^{-1} sampled. The expected error bars can be seen on the right side of Figure 26. More likely, we will be able to use events from the entire collision vertex, resulting in the error bars shown in Figure 27 from the combined Run-11 and Run-12 data sets. It is clear that the 500 GeV data from PHENIX will have a substantial impact; Run-11 alone will be important once the signal to background ratio is optimized.

The plots in Figure 28 show the current uncertainties obtained by a pQCD fit[17] to the world data from inclusive and semi-inclusive deep inelastic scattering. Figure 29 shows the impact of the W$^{\pm}$ A_L for 300 pb^{-1} with a mean polarization of 60%. The W data reduce the uncertainties on the sea-quark polarizations for $0.05 < x < 0.6$ significantly. Furthermore, the RHIC W-program provides a completely complementary theoretical approach to calculate these pdfs, and therefore an important cross check of the pQCD formalism used to describe semi-inclusive data.

Our main tool, in the short run, for constraining the gluon contribution to the proton spin will continue to be $A_{LL}^{\pi^0}$. As is shown in Figure 30, 500 GeV collisions provide access

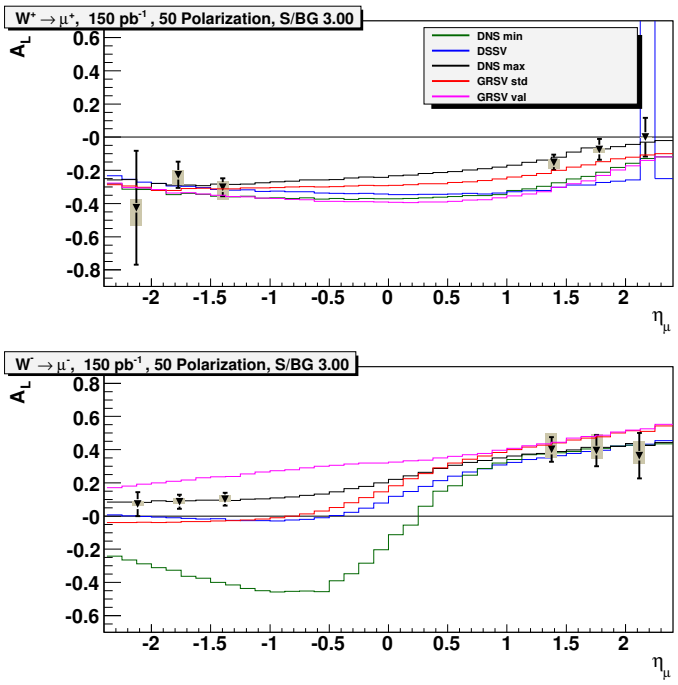

Figure 27: Expectation for uncertainties in W asymmetry measurements with 150 pb^{-1} recorded with 50% polarization and S/B=3.0.

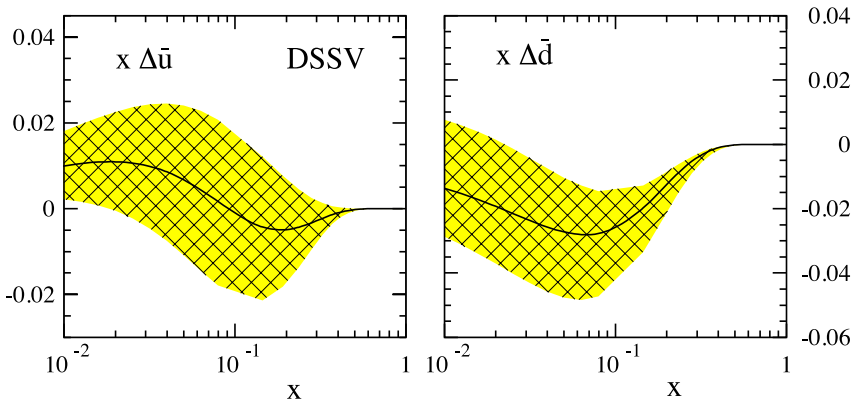

Figure 28: Uncertainty band on $x\Delta\overline{u}$ and $x\Delta\overline{d}$ resulting from the current fit to the world data from inclusive and semi-inclusive DIS by DSSV[17].

to a lower x range than at 200 GeV.

Figure 31 shows the expected uncertainties in $A_{LL}^{\pi^0}$ as a function of p_T at 500 GeV assuming we reach 50 pb¹ recorded in Run-11 within the standard ±30 cm vertex and a polarization of 50%. The calculation is for π^0 measured in the PHENIX central arms. As there is considerable material thickness due to the vertex detector support structure beyond the ±10 cm vertex region, the estimation is based on only 18 pb^{-1} within ±10

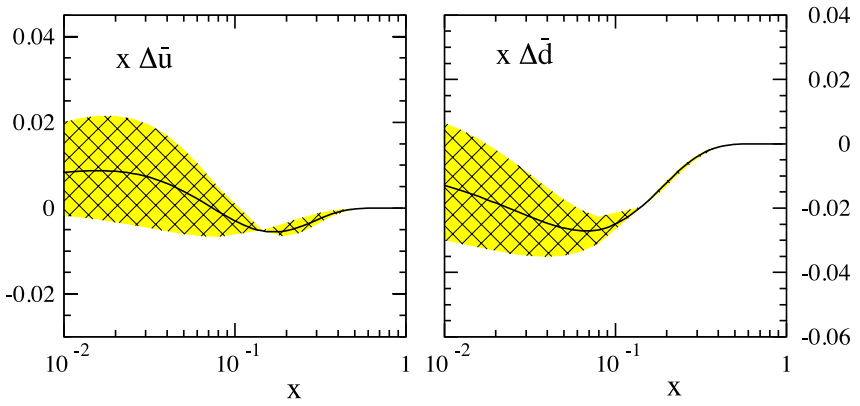

Figure 29: Improvement in the uncertainties in Figure 28 with added constraint from W±A_L measured with 300 pb−1 of 500 GeV p+p collisions with 60% polarization.

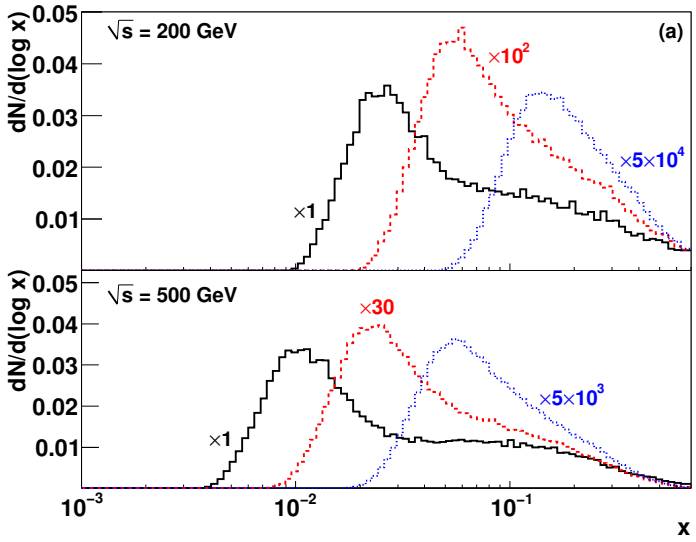

Figure 30: x range covered by π^0 at different p_T in 200 and 500 GeV collisions. Black, red, and blue curves correspond to 2-2.5, 4-5, and 9-12 GeV/c p_T, respectively.

cm. We will also utilize π^0 reconstructed in the Muon Piston Calorimeter (MPC), which will increase the reach to smaller x. As this is a double spin asymmetry, it is important to have the highest polarization achievable; the difference between 50% (40%) and 60% polarization is the equivalent to recording more than a factor of two (five) times higher luminosity.

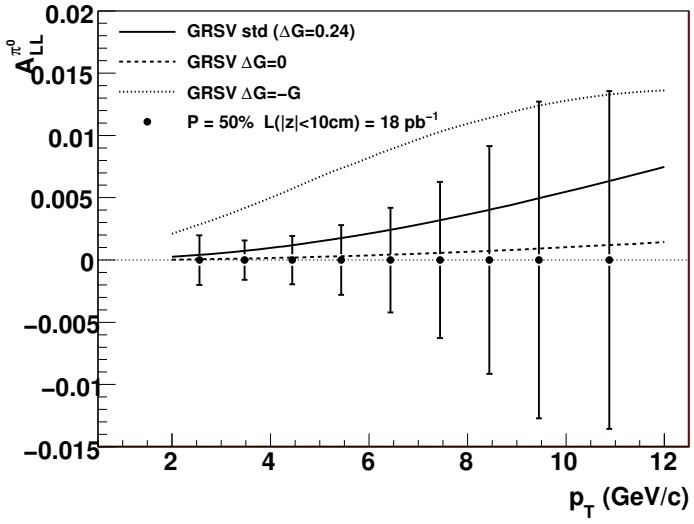

Figure 31: Expected uncertainties in $A_{LL}^{\pi^0}$ as a function of p_T in Run-11. Only collisions with vertex inside ± 10 cm are included.

5.3.2 200 GeV Au+Au collisions

The PHENIX experiment with the VTX will open a new window for understanding partonic energy loss in the quark gluon plasma. In so doing, it will give perhaps some of the best constraints on fundamental medium properties including the shear viscosity to entropy density ratio (η/s). Consistent with last year's beam-use proposal for Run-11, PHENIX requests 8 weeks of physics running for Au-Au collisions at $\sqrt{s_{NN}} = 200$ GeV. We note that this was one of the top priorities in the recommendations from the NPP Program Advisory Committee last year, specifically to "exploit the capabilities of the PHENIX VTX detector" [25]. The new VTX detector will allow separate measurements of the charm and bottom nuclear modification factors (R_{AA}) and provide first elliptic flow measurements for hadrons containing charm and bottom quarks; this is achieved by measuring single displaced vertex electrons.

The PHENIX experiment was specifically designed for exceptional electron identification in the high multiplicity environment of central Au-Au reactions. In 2007, PHENIX published our Run-04 Au-Au results on non-photonic electrons in Physical Review Letters [26]. As shown in Figure 32, the measurements of the nuclear modification factor out to $p_T \approx 10$ GeV/c and elliptic flow v_2 indicate a dramatic change in the momentum distribution of heavy quarks in the medium. This Letter has over 200 citations in the last three years as a rough indicator of the interest in the field in these results. In a recent manuscript submission, we provide substantial details (with 48 pages) on the entire analysis procedure, systematic uncertainty estimation, and theoretical model comparisons [22]. As shown in Figure 33, these results present a challenge for the the perturbative (weak

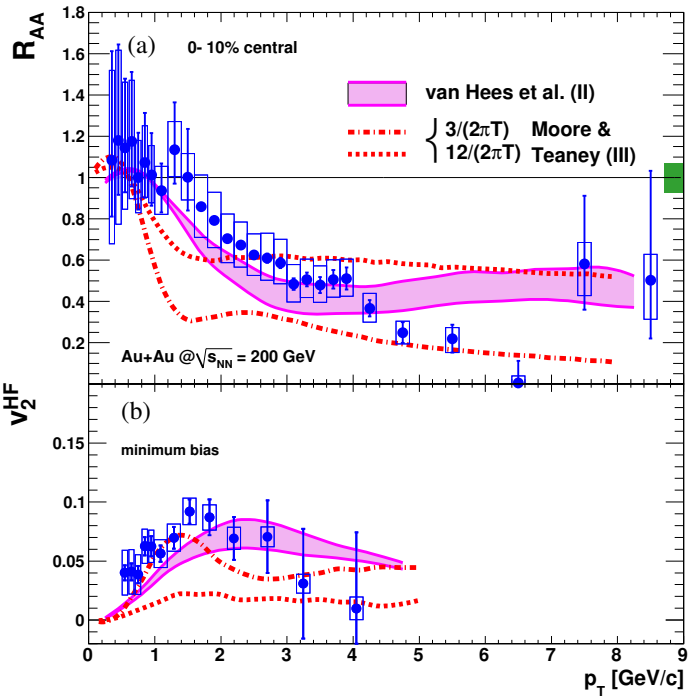

Figure 32: (a) RAA of heavy-flavor electrons in 0-10% central collisions compared with PHENIX π^0 data and various model calculations. The box at $R_{AA} = 1$ shows the uncertainty in the number of binary collision estimate. (b) v_2 of heavy-flavor electrons in minimum bias collisions compared with PHENIX π^0 data and the same models.

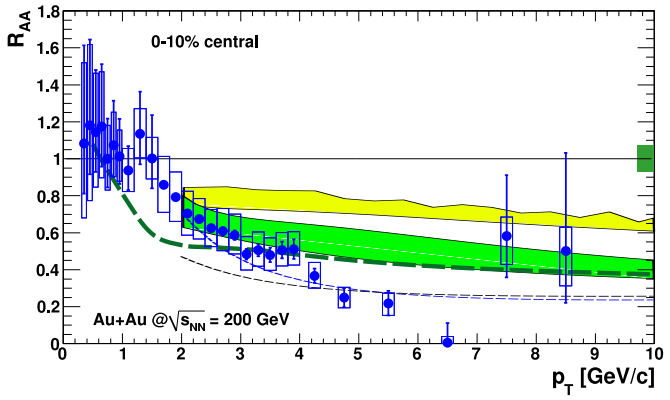

Figure 33: R_{AA} in 0-10% centrality compared with energy loss models. The thick dashed curve is the BDMPS calculation for electrons from D and B decays. The bands are DGLV calculations for electrons from D and B decays. The lower band contains collisional energy loss as well as radiative energy loss. The thin dashed curves are DGLV calculations for electrons from D decays only.

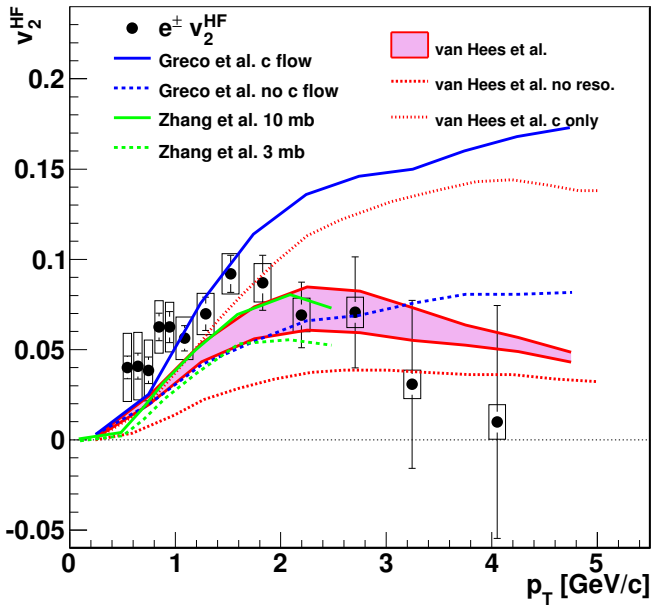

Figure 34: Non-photonic electron (HF) elliptic flow (v_2) as a function of transverse momentum compared with theoretical models from Greco et al., Zhang et al., and van Hees et al.

coupled expansion approximation) picture of partonic energy loss. However, the key issue is that the non-photonic electrons have contributions from both charm hadron (e.g. D meson) and beauty hadron decays. It is expected that charm hadrons dominate the electron contribution for $p_T < 5$ GeV/c and beauty hadrons for $p_T > 5$ GeV/c. This is roughly confirmed by examining non-photonic electron - hadron angular correlations in proton-proton reactions [23]. However, statistical uncertainties are large and the current perturbative QCD FONNL calculations have an uncertainty in the ratio of $(b \longrightarrow e)/(c \longrightarrow e)$; the ratio is approximately 0.5 ± 0.2 at $p_T = 5$ GeV/c. Furthermore, the production cross sections must be measured in Au+Au collisions directly, rather than inferred from p+p collisions or theory.

Additionally, as shown in Figure 34, some calculations of charm quark flow in the quark gluon plasma indicate a flow approaching 20% at $p_T = 5$ GeV/c. Despite large statistical uncertainties for $p_T > 2.5$ GeV/c, the data do not support a continued flow increase. However, this may or may not be due to the predominance of beauty quark contributions (which cannot be presently determined given the large uncertainty on the b/c fraction.

The measurements with the VTX detector will unambiguously resolve these puzzles. Expectations are that the beauty quarks are so heavy, that in a diffusion calculation they

should be difficult to move around. Consequently, they should exhibit minimal flow. In the perturbative energy loss framework, radiative energy loss via gluon bremstrahhlung is suppressed due to the "dead cone" effect (where forward radiation is limited for heavy quarks traveling at velocities much less than the speed of light). If in fact the beauty quarks exhibit strong suppression in the medium, this challenges the entire paradigm of perturbative energy loss as the right framework for understanding jet quenching. Additionally, the charm flow out to higher p_T (as separated from beauty flow) may well provide one of the best constraints on the η/s ratio via diffusion calculations. This provides an excellent alternative methodology to the bulk flow of light hadrons in comparison to viscous hydrodynamic models for constraining this quantity and answering the question of how close to the conjective minimum bound the quark gluon plasma at this temperature is.

What answers can we expect with an 8 week Au-Au run at 200 GeV Run-11? CAD projects a peak luminosity in Run-11 of $40 \times 10^{26} cm^{-2} s^{-1}$ and an average store luminosity of $20 \times 10^{26} cm^{-2} s^{-1}$. The VTX detector spans a range along the beam axis from -10.0 cm to +10.0 cm. Thus, collisions that occur outside this narrow region will produce particles that have a much smaller acceptance for hits in the VTX, in addition to encountering almost a full one radiation length of material (the support structure and readout for the VTX). The fraction of all collisions expected within this narrower z-vertex range is approximately 25% (which was achieved in Run-10).

In Run-10, the PHENIX Data Acquisition system was able to record 5 kHz of minimum bias Au-Au events. The VTX detector installation is also coupled with new data acquisition electronics (the Data Collection Module II) and upgrading the Event Builder switch (as part of the PHENIX DAQ/Trigger 2010 project). The upgrades for reading out the VTX have full capabilities in significant excess of 5 kHz; however, this will be the first running period for the VTX and the new data acquisition hardware and will require commissioning time and periods with rates below the ultimate performance specifications. Thus, the data acquisition experts have estimated an average data taking rate of 2.5 kHz during this first running period (with the possibility for improved performance during the run). At this rate, we are limited by the beam luminosity during the first few weeks of ramp-up, and data acquisition rate limited thereafter (assuming only the 2.5 kHz rate). Thus, we estimate that after 2 weeks of setup and for 8 weeks of physics data taking, we would record 4.7 billion minimum bias Au-Au events at full energy.

We show the projected performance uncertainties from 4.7 billion minimum bias Au-Au events (or as a subset 0.47 billion 10% central Au-Au events). Shown in Figures 35 and 36 are the p_T distributions of heavy flavor electrons from charm and beauty hadrons and the corresponding nuclear modification factors. Note that the nuclear modification factors will also require running p+p collisions at $\sqrt{s} = 200$ GeV with the new detectors. Figure 37 shows the projected uncertainties for minimum bias Au-Au collisions for the elliptic flow observables. These initial results will provide great insight into the interaction of heavy

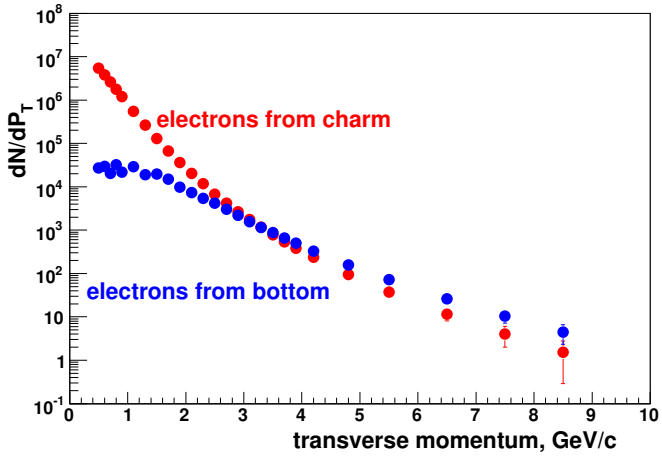

Figure 35: Shown are the projected uncertainties for the transverse momentum distribution for heavy flavor electrons tagged with a displaced vertex from charm hadron decay (red) and beauty hadron decay (blue). The uncertainties are for 10% central Au-Au reaction as a subset of a total of 4.7 billion Au-Au minimum bias events.

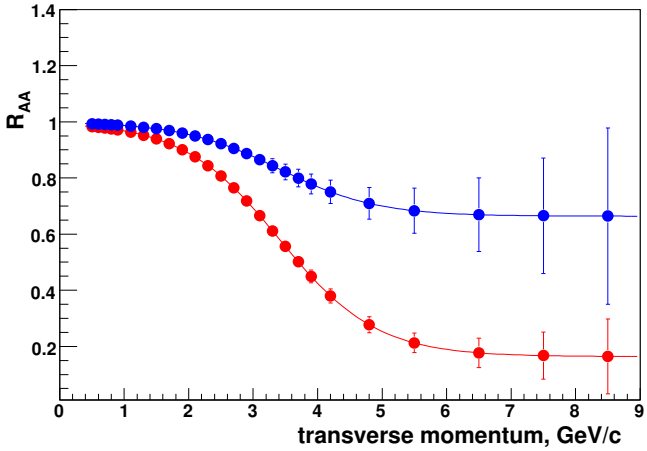

Figure 36: Shown are the projected uncertainties for the nuclear modification factor (R_{AA}) as a function of transverse momentum for heavy flavor electrons tagged with a displaced vertex from charm hadron decay (red) and beauty hadron decay (blue). The uncertainties are for 10% central Au-Au reaction as a subset of a total of 4.7 billion Au-Au minimum bias events.

flavor quarks in the medium. For the elliptic flow projections, we have assumed a reaction plane resolution comparable to that from the reaction plane detector that was installed prior to Run-07. This detector has to be removed prior to Run-11 due to conflicting space requirements with the VTX, but studies indicate that the MPC, VTX(and later in Run-12 the FVTX) can be similarly utilized with a comparable resolution.

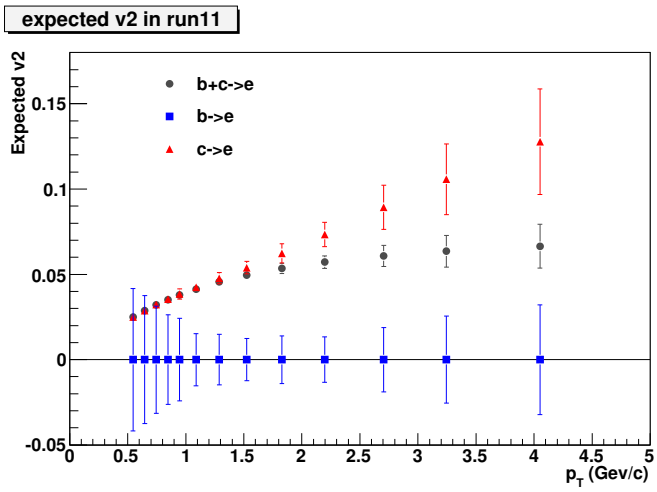

Figure 37: Shown are the projected uncertainties for the elliptic flow v_2 as a function of transverse momentum for heavy flavor electrons tagged with a displaced vertex from charm hadron decay (red) and beauty hadron decay (blue). The uncertainties are for 10% central Au-Au reaction as a subset of a total of 4.7 billion Au-Au minimum bias events.

5.3.3 Au+Au at $\sqrt{s}$=27 and 18 GeV

As shown above, Run-10 provided a good start on the energy scan at RHIC. The PHENIX Collaboration is enthusiastic to complete the first part of this scan by collecting data at additional points between full RHIC energy and that studied at the SPS. The goals for these data are twofold: one is to search for evidence of the QCD critical end point, and the other is to search for the onset of the perfect liquid, i.e. a liquid which flows with negligible viscosity to entropy ratio. A minimum shear viscosity is indicative of phase transitions in various strongly coupled systems[27, 28]. Consequently, the study of elliptic flow of identified hadrons is the key observable for viscosity studies.

Measurement of the elliptic flow of pions, kaons and protons will show whether the scaling of v_2, which was shown to hold for high $\sqrt{s}$ collisions is broken. The magnitude of v_2, along with its centrality and p_T dependence are the main observables which constrain hydrodynamics calculations (we note that hadron p_T spectra are also important, but they do not pose a significant running time requirement compared to elliptic flow measurements). Comparison of 3-d hydro calculations, especially the trends with centrality and p_T are important to extracting the viscosity to entropy ratio, η/s from the data, utilizing the new approaches, codes, and results being developed by theorists in the TECHQM collaboration. Hydrodynamics calculations constrained to reproduce the bulk matter flow are also of key importance to extraction of the initial temperature of the perfect fluid from the observed photon spectrum.[19]

Observation of the breaking of constituent quark scaling of the elliptic flow would

signal deviation from the partonic-level flow patterns observed at high RHIC energy. This, in addition, to increased viscosity/entropy would signal that the plasma phase no longer dominates the flow. The critical end point search requires measurement of particle production ratios, spectra and fluctuation analyses, which has smaller event number requirements.

In order to evaluate the running time required for these measurements, we utilize RHIC luminosity projections from Wolfram Fischer (private communication), along with the following assumptions:

- RHIC uptime = 55%
- PHENIX uptime at low energy = 77%
- No storage RF, consequently the collision vertex is elongated causing an effective luminosity loss of a factor of two inside a finite vertex cut
- 25% of the collisions fall inside a vertex cut of ± 30 cm, and 8% fall inside 10 cm.

Table 4: Collision rates for low energy Au+Au and p+p

$\sqrt{s_{NN}}$	**ave.lumi.** ($cm^{-2}sec^{-1}$)	σ **(b)**	**Events/Day in 30 cm**	**Events/Day in 10 cm**
Au+Au				
18	6.00 E+25	6.8	3.73 M	1.24 M
27	8.00 E+25	6.8	4.98 M	1.66 M
p+p				
22	2.50 E+29	0.03	68.6 M	22.9 M
27	6.00 E+29	0.032	176 M	58.5 M
39	2.40 E+30	0.033	724 M	241 M
62	4.80 E+30	0.0356	1.56 B	521 M

The resulting expected data rates are listed in Table 4. In one week of running Au+Au at 27 GeV, PHENIX would collect approximately 35 million events with vertex inside ±30 cm and 11.6 million events in ±10 cm. In 1.5 weeks (10 days) of Au+Au at 18 GeV, the event samples would be 37 million events in ±30 cm and 12.4M events in ±10 cm.

We quote both values because once the VTX is installed, there is a significant amount of material introduced outside of 10 cm in the VTX support structure. Consequently, it may be that the identified hadron analysis will only use events with vertex in the central 10cm; we will not be certain of this until we are able to look at the data.

Figure 38 shows the expected error bars on the measurement of v_2 per quark as a function of p_T per quark. The top row shows results for 27 GeV Au+Au, and the bottom

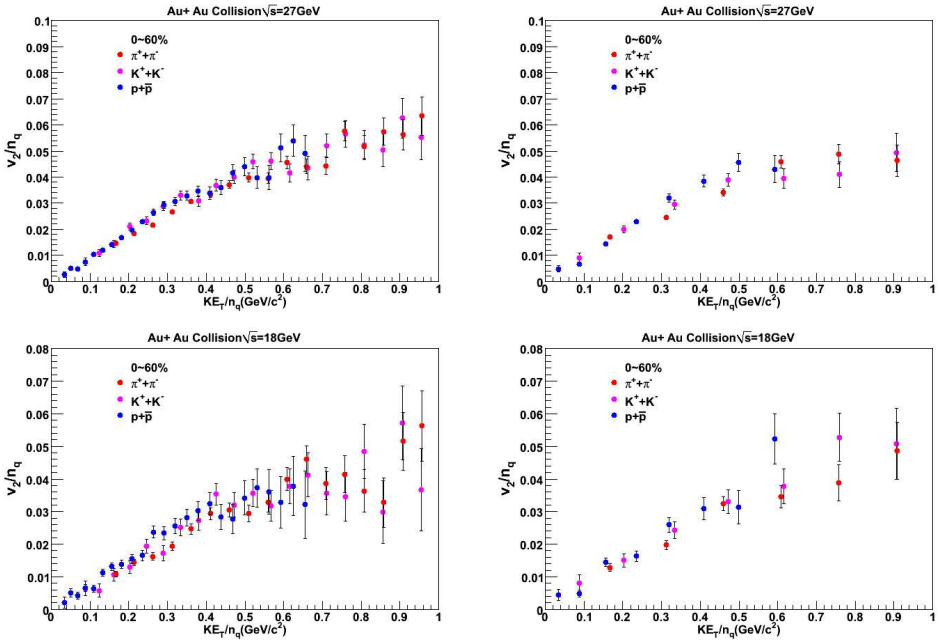

Figure 38: Projected v_2 per quark as a function of p_T per quarks for 27 GeV Au+Au (top) and 18 GeV Au+Au (bottom). The left side shows results for 30 million events and the right for 10 million events. All projection are for 0-60% centrality.

for 18 GeV. The left side shows the projected performance with 30M events inside a 30 cm vertex cut, while the right side shows projections for 10M events, which would result with a 10cm vertex cut. All plots are for nearly minimum bias samples (0-60% centrality). It is clear that PHENIX will have good sensitivity to detect breaking of v_2 scaling at 27 GeV. At 18 GeV the sensitivity is also good if the entire $\pm$30 cm vertex region can be used. Limitation to 10 million events would degrade the sensitivity above transverse kinetic energy per quark of 0.5 GeV/c^2. We note that these simulations took into account the removal of the reaction plane detector (RXNP) to make room for the VTX. In Run-11 the reaction plane will be determined by the MPC and VTX detectors. Guided by measured performance at higher energies, the calculation in Figure 38 was done assuming reaction plane resolution of 25% at 18 GeV and 34% at 27 GeV.

5.3.4 p+p comparison data at low energy

In Run-10 PHENIX collected 700M and 250M events of Au+Au data at $\sqrt{s_{NN}}$=62.4 and 39GeV, respectively. A first look at the data indicates that the accessible p_T range for π^0 reaches 8 GeV/c and 10 GeV/c respectively, requiring least 10 counts in the last 1 GeV/c wide bin (31% stat. error). Raw yields representing approximate 2/3 of the available statistics are shown on Fig. 39 and Fig. 40. The main objective of the measurement is

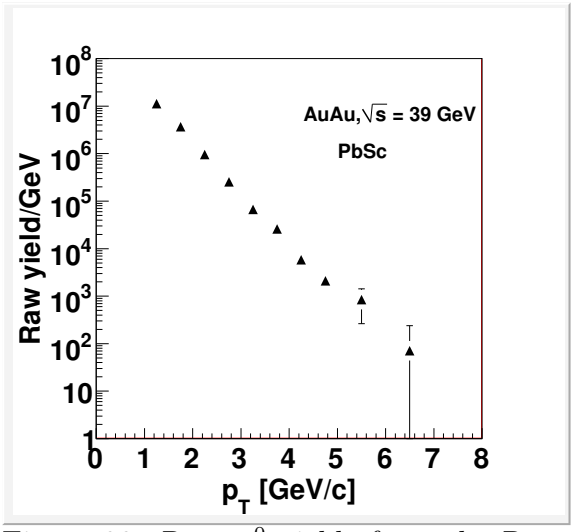

Figure 39: Raw π^0 yields from the Run-10 39GeV AuAu data, representing about 2/3 of the statistics.

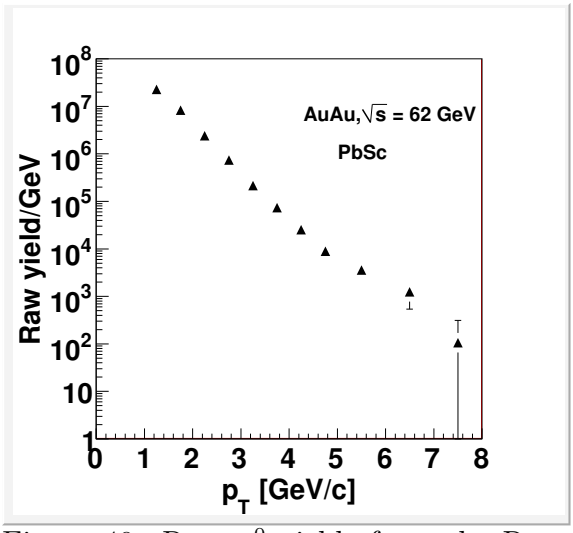

Figure 40: Raw π^0 yields from the Run-10 62GeV AuAu data, representing about 80% of the statistics.

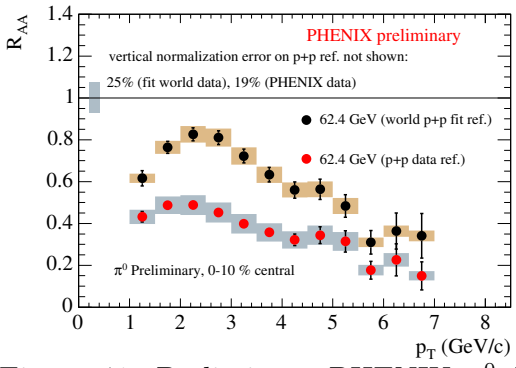

Figure 41: Preliminary PHENIX π^0 R_{AA} in central 62 GeV Au+Au collisions using a fit to the world average of previous pp data (black circles) and a PHENIX pp measurement (red circles).

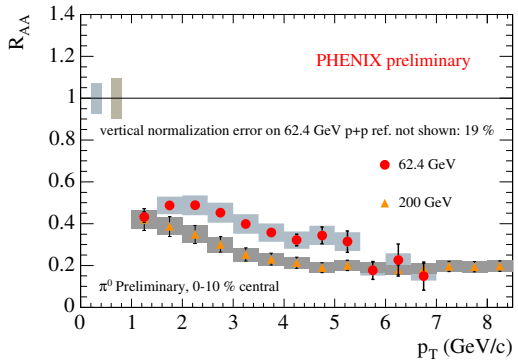

Figure 42: Preliminary PHENIX π^0 R_{AA} in central 62 GeV (red circles) and 200 GeV (orange triangles) Au+Au collisions. Both ratios use PHENIX pp measurements.

to establish the evolution of the nuclear modification factor R_{AA} which in turn needs reference spectra from p+p collisions at the same $\sqrt{s}$.

Reference data from the same experiment is key for this observable. This was seen in the initial Run-4 measurement of π^0 suppression in Au+Au at $\sqrt{s_{NN}}$=62GeV, using a weighted average of the existing world data [29]. Two years later PHENIX collected reference (p+p) data and re-calculated R_{AA}. The results are shown in Fig. 41 and the physics message is clearly completely different. As shown in Fig. 42 when using our own

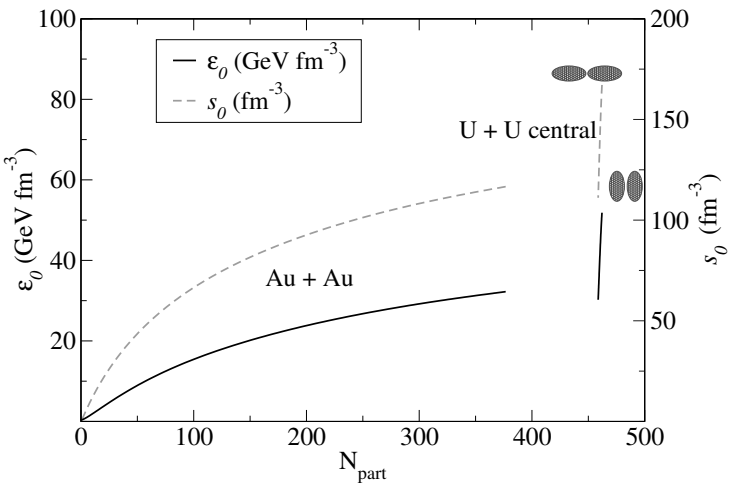

Figure 43: Energy density and entropy density as a function of the number of participating nucleons for Au-Au and U-U collisions. Figure reproduced from [30].

reference the suppression is almost as large as at 200GeV.

The existing PHENIX 62 GeV p+p π^0 data (from Run-6 with 0.1 pb^{-1}) [11] barely reach p_T = 7GeV/c [16]. In Run-4 Au+Au at 62 GeV, PHENIX collected 58M events or 0.36pb^{-1} pp-equivalent. In Run-10, there are at least 300M useful physics events at 62 GeV. Consequently, approximately 1.9 pb^{-1} of p+p collisions are required for a measurement of direct photon R_{AA}. For $\pi^0 R_{AA}$, about a quarter of this suffices. From Table 4 one can see that 1.0 pb^{-1} could be collected in approximately 12 days.

In 39 GeV Au+Au in Run-10, the π^0 analysis utilizes a data set, corresponding to somewhat more than 1 pb^{-1} p+p-equivalent luminosity. Consequently we require at least 0.5pb^{-1} p+p data to utilize the entire available p_T range. From Table 4 one can see that 0.5 pb^{-1} could be collected in approximately 12 days.

If one can interpolate the π^0 yield at some energies, then the most important measurement to make is at 22 GeV, which is the lowest energy at which PHENIX has measured π^0 suppression. Data at this energy will avoid extrapolation, and provide a good anchor for interpolation of points between 22 and 62 GeV. In order for the p+p statistical uncertainty to match that in 22 GeV Cu+Cu, 0.01 pb^{-1} are required. With the VTX in place, useful events must have vertices inside 10cm to avoid conversion of π^0 decay photons in the VTX support material. Collecting such a data set requires running for approximately 6 days. Adding the changeover time means that this run would require one week.

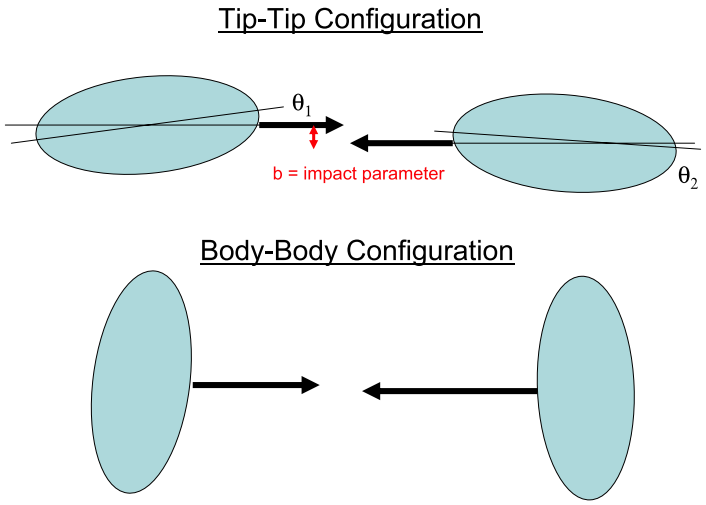

Figure 44: Uranium-Uranium geometry picture showing the tip-tip configuration (top) and the body-body configuration.

5.3.5 U+U at $\sqrt{s} = 192.8$ GeV

There is significant anticipation for the availability of Uranium beams at RHIC. The key physics interest arises from the significant deformation of Uranium nuclei (non-sphericity). It has been calculated that in tip-tip collisions (as illustrated in Figure 1), a higher energy density (as shown in Figure 43) is achieved. Probing this higher energy density can provide key tests of hydrodynamic behavior and the path-length dependence of parton energy loss [30]. More recently, it has been proposed [31] that body-body collisions (as illustrated in Figure 1) may be an excellent test of the hypothesized local parity violating bubbles. These collisions near impact parameter $b = 0$ should have zero magnetic field and thus no charge separation effect related to local parity violation, while the overall eccentricity remains large (thus allowing one to examine competing flow and fluctuations effects). The key to utilizing Uranium collisions for these purposes is the ability to disentangle the various geometries of the individual interactions. For two spherical nuclei, one impact parameter value (b) determines the initial nuclear geometry (and then fluctuations of the nucleon positions within each nuclei). However, in Uranium collisions, in addition to the impact parameter, the two nuclei have rotations in spherical coordinates$(\theta_1, \phi_1, \theta_2, \phi_2)$. Numerous papers have made proposals for separating these various geometries [32, 33, 34, 35].

In order to study and reproduce some of these proposed methods, we have modified the PHOBOS Glauber Monte Carlo [36] (as publicly available at http://projects.hepforge.org/tglaubermc/) to include the Uranium geometry following the prescription in [32] and also the forward neutron distribution (for modeling the response in the Zero Degree Calorimeters). If

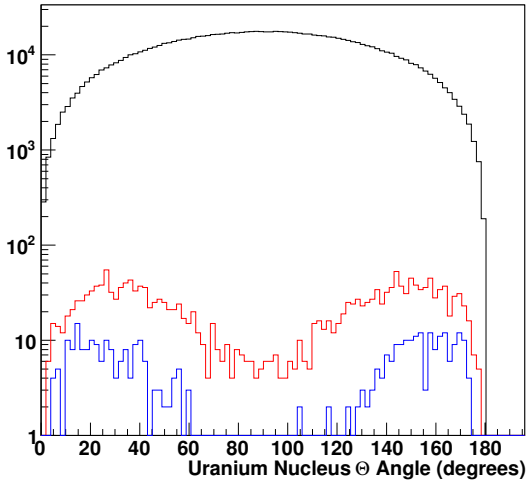

Figure 45: Glauber Monte Carlo results for Uranium-Uranium collisions for the θ angle of one nucleus. The black histogram is all collisions (i.e. random geometry), the red curve is selecting the highest 0.2% based on charged particle multiplicity (assuming the two-component model) and the blue curve is selecting the highest 0.04%.

the charged particle multiplicity $dN_{ch}/d\eta$ at mid-rapidity is correctly described by the two-component model (as discussed in [35]) where:

$$\frac{dN_{ch}}{d\eta} \propto (1 - X_{hard}) \times \frac{N_{part}}{2} + X_{hard} \times N_{binary} \quad (1)$$

then the very highest multiplicity events can simply be selected with a highly enhanced tip-tip contribution. However, the two-component model yields 10% discrepancies when comparing Au-Au to Cu-Cu reactions and alternative scalings have also been successful. It is notable that in [37] they discuss Uranium geometries in terms of gluon saturation effects and find a smaller selectability in these highest multiplicity events. An initial data sample is necessary in order to test these various pictures (which is of physics interest in its own right), to then understand how the geometry can be disentangled. The selectivity within the two-component model alone and a cut on charged particle multiplicity for the top 0.2% and 0.04% is shown in Figure 45. The angular selection for the tip-tip configuration remains rather broad.

Additional proposals have been made that one can select event categories by a combination of elliptic flow and multiplicity or zero degree energy. For tip-tip collisions, the eccentricity is small and thus the elliptic flow (v_2) should be small. However, this becomes quite complicated for some of the physics goals (for example testing the limits of the hydrodynamical models) because one has used a specific observable of interest to

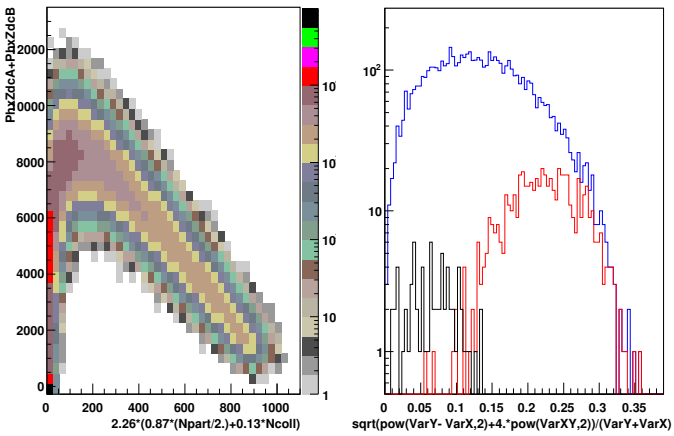

Figure 46: Shown in the left panel is the modeled distribution for charged particle multiplicity (based on the two-component model) versus the zero degree energy. In the right panel we have selected the smallest 0.6% impact parameter events based on the left panel distribution and we show the participant eccentricity (ϵ_{part}) distribution for these events. In black are the events aligned within 30 degrees of tip-tip (and one can see the preference for small eccentricity) and in red are the events aligned within 30 degrees of body-body (and one can see the preference for larger eccentricty and for $\epsilon_{part} > 0.25$ this dominates the sample).

hydrodynamics in the event selection; this can produce a bias. Alternatively, body-body collisions might be selected by looking for almost no zero degree energy and then large eccentricity via large v_2. However, PHENIX finds that even in the most central Au-Au reactions, there is still non-zero energy in the zero degree calorimeters. This is likely due to a few percent probability to have the nucleons interact, but charge exchange a proton to a neutron or have a very small angle scatter of the initial neutron. Shown in Figure 46 (left panel) is the modeled distribution for charged particle multiplicity (based on the two-component model) versus the zero degree energy. We select the $dN_{charge}/d\eta > 700$ and $ZDC_{energy} < 1500GeV$ (corresponding to 0.6% of the total cross section), and find that almost all such events have impact parameter $b < 2$ fm. In Figure 46 (right panel) we show the participant eccentricity (ϵ_{part}) distribution for these events. In black are the events aligned within 30 degrees of tip-tip (and one can see the preference for small eccentricity) and in red are the events aligned within 30 degrees of body-body (the preference for larger eccentricty and for $\epsilon_{part} > 0.25$ this dominates the sample). There are many model assumptions that go into this calculation that need validation with real data, but the results show promise. Consequently, the PHENIX Beam Use Proposal supports a modest commissioning run, with the possibility for longer running in the coming physics runs.

The Electron Beam Ion Source (EBIS) is expected to be available for commissioning

in the fall of 2010 (for the RHIC Run-11 running period). EBIS will provide a new heavy ion pre-injector for RHIC based on a high charge state heavy ion source, a Radio Frequency Quadrupole (RFQ) accelerator, and a short Linear Accelerator. EBIS has the potential for significant future intensity increases and can produce heavy ion beams of all species including uranium (that has been previously unavailable). In the most recent "RHIC Collider Projections (FY 2011- FY 2015)" dated May 11, 2010, the stated luminosity average for a store is $8 \times 10^{26} cm^{-2} s{-}1$ corresponding to an interaction rate of approximately 5.5 kHz. Since the β^* is quoted at 0.65 meters, we assume that 55% of collisions will take place within the z-vertex ($|z| < 30$ cm) and 30% within the z-vertex ($|z| < 10$ cm), corresponding to average interaction rates of 3.0 kHz and 1.6 kHz respectively. For most of the physics of interest in a short Uranium-Uranium run, the full acceptance of the new silicon vertex detector (VTX) is necessary. Consequently, we will primarily focus on the narrowest z-vertex range. In the projections document, it states that at the end of the initial ramp-up period the luminosities may be "lower than at the end of the running period by a factor of 2-4" (where the above numbers were "after a sufficiently long running period."). Thus, for planning purposes, we will assume during a short initial commissioning run a factor of 3 lower rate, resulting in 530 Hz of U-U interactions within $|z| < 30$ cm.

In a period with 0.5 weeks setup for U-U (after full energy Au-Au running) followed by 1.5 weeks of data taking, PHENIX can record $\mathbf{150 - 200}$ million minimum bias U-U interactions. A 200 million event data sample would yield approximately 400,000 events in the tip-tip configuration, corresponding to approximately 0.2% of the cross section. This should be sufficient for geometry studies. Note that if one could perfectly select events with impact parameter $b < 2$ fm and with both nuclei aligned within less than 30 degrees of the tip-tip configuration, this corresponds to only 0.03% of the total cross section. Given the rate estimates for this commissioning run, measurements for these configurations involving rare probes or high p_T will not be possible.

Based upon these considerations, we request 0.5 + 1.5 week for commissioning the Uranium beam collisions and followed by collection of the data samples necessary to study the various geometry issues.

5.4 Run-12

As for Run-11, PHENIX has a dual top priority in Run-12 of completing collection of 150 pb$-$1 of 500 GeV p+p collisions and full energy Au+Au running to utilize the new FVTX detector, which will be installed prior to Run-12. The W asymmetry measurement performance for the combined Run-11 and Run-12 is shown in Figure 27 above. While this study conservatively assumed 50% polarization in both Run-11 and Run-12, improved performance would substantially improve the figure of merit of the measurement.

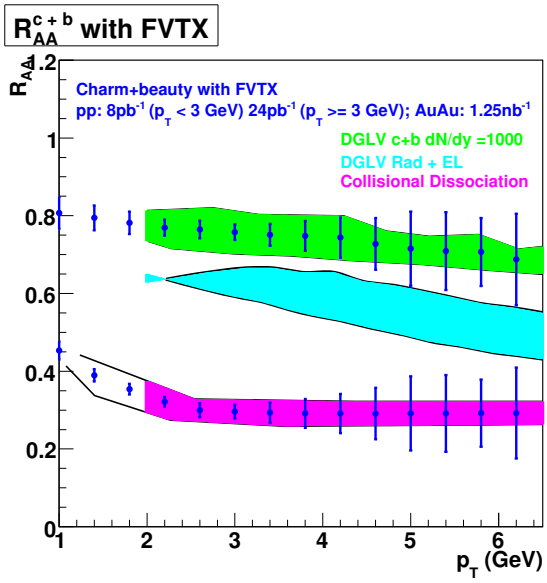

Figure 47: Simulated performance for measurement of R_{AA} of muons from heavy flavor decays at forward rapidity. Fully simulated FVTX detector performance for tagging displaced vertices, along with 1.25 nb^{-1} of 200 GeV Au+Au and 24 pb^{-1} of 200 GeV p+p collisions are assumed. .

The FVTX, in conjunction with the muon arms, will allow measurement of single muons from c and b decays. The expected error bars on forward heavy flavor R_{AA} is shown in Figure 47 for $\sqrt{s_{NN}}$=200 GeV Au+Au integrated luminosity of 1.2 nb^{-1}. The figure shows that the measurement will provide excellent discriminating power for the role of collisional dissociation in the energy loss mechanism for heavy quarks. While it is too soon to realistically demonstrate that a data set of this magnitude can be collected in one year, particularly in the first year the detector is commissioned, we envision that a first measurement of heavy flavor decay muons from a subset of this data will be valuable in its own right. The ultimate measurement is envisioned to result from combining data from two Au+Au runs, and using as reference 24 pb^{-1} of 200 GeV p+p data, which we envision collecting in Run-13.

Our next priority for Run-12 is to complete the energy scan physics by collecting the missing p+p reference data at lower energy. The specific request is detailed above.

References

[1] Initial PHENIX Run-1 request, 24-May-99, http://www.phenix.bnl.gov/phenix/WWW/publish/zajc/sp/presentations/RBUP99/rbup99.htm

[2] PHENIX Run-1 presentation to PAC, 23-Mar-00, http://www.phenix.bnl.gov/phenix/WWW/publish/zajc/sp/presentations/ RBUP00/rbup00.htm

[3] PHENIX Run-2 presentation to PAC, http://www.phenix.bnl.gov/phenix/WWW/publish/zajc/sp/presentations/ RBUP-Nov00/RBUPNov00.htm

[4] PHENIX Run-2 proposal for extended running: http://www.phenix.bnl.gov/phenix/WWW/publish/zajc/sp/presentations/ RBUPSep01/RBUPSep01.html

[5] PHENIX Runs 3-5 proposal to PAC, Aug-02, http://www.phenix.bnl.gov/phenix/WWW/publish/zajc/sp/presentations/ RBU-PAug02/RBUPforAug02PAC.pdf

[6] PHENIX Beam Use Proposal for RHIC Runs 4-8, Sep-03, http://www.phenix.bnl.gov/phenix/WWW/publish/zajc/sp/presentations/ RBUP03/ProposalText/RBUPforRuns4-8.pdf

[7] PHENIX Beam Use Proposal for RHIC Runs 5-9, Jul-04, http://www.phenix.bnl.gov/phenix/WWW/publish/zajc/sp/presentations/ RBUP04/ProposalText/RBUPforRuns5-9.pdf

[8] PHENIX Beam Use Proposal for RHIC Run-6 and Beyond, Oct- 05, http://www.phenix.bnl.gov/phenix/WWW/publish/zajc/sp/presentations/ RBUP05/ProposalText/RBUPforRun7andBeyond.pdf

[9] PHENIX Beam Use Proposal for RHIC Run-7 and Beyond, Sep- 06, http://www.phenix.bnl.gov/phenix/WWW/publish/zajc/sp/presentations/ RBUP06/ProposalText/RBUPforRun7andBeyond.pdf

[10] PHENIX Beam Use Proposal Update for RHIC Run-7 and Beyond, Mar-07, http://www.phenix.bnl.gov/phenix/WWW/publish/jacak/sp/ RBUP07/RBUP07_update.pdf

[11] PHENIX Beam Use Proposal for RHIC Run-9 and Beyond, April- 08, http://www.phenix.bnl.gov/phenix/WWW/publish/jacak/sp/BeamUse08/ RBUP08_proposal.pdf

[12] PHENIX Beam Use Proposal for RHIC Run-10 and Run-11, June 09, http://www.phenix.bnl.gov/phenix/WWW/publish/jacak/sp/BeamUse09/ RBUP09.pdf

[13] Research Plan for Spin Physics at RHIC, submitted to U.S. Department of Energy February, 2005, available from http://spin.riken.bnl.gov/rsc/report/masterspin.pdf

[14] Plans for the RHIC Spin Physics Program, submitted to U.S. Department of Energy June, 2008; available from http://spin.riken.bnl.gov/rsc/report/spinplan_2008/spinplan08.pdf

[15] A. Adare *et al.* (PHENIX Collaboration), Phys. Rev. Lett. **103**, 012003(2009).

[16] A. Adare *et al.* (PHENIX Collaboration), Phys. Rev. D**79**, 012003 (2009).

[17] Daniel de Florian, Rodolfo Sassot, Marco Stratmann and Werner Vogelsang, Phys. Rev. Lett. **101**, 072001 (2008).

[18] G. Bunce, N. Saito, J. Soffer and W. Vogelsang, Ann. Rev. Nucl. Part. Sci. **50**, 525 (2000), hep-ph/0007218.

[19] A. Adare *et al.* (PHENIX Collaboration), Phys. Rev. Lett. **104**, 132301(2010).

[20] A. Adare *et al.* (PHENIX Collaboration), Phys. Rev. C**81**, 034911(2010).

[21] R. Rapp and H. van Hees, Phys. Rev. C**63**, 054907 (2001); nucl-th/0204003; and private communication.

[22] A. Adare *et al.* (PHENIX Collaboration), arXiv:1005.1627, submitted to Phys. Rev. C. (2010).

[23] A. Adare *et al.* (PHENIX Collaboration), Phys. Rev. Lett. **103**, 082002 (2009).

[24] RHIC Collider Projections (FY2009-FY2013), W. Fischer *et al.*, last updated May 11, 2010, available from http://www.agsrhichome.bnl.gov/RHIC/Runs/RhicProjections.pdf

[25] http://www.bnl.gov/npp/docs/pac0609/FinalRecommendations(20.pdf

[26] A. Adare *et al.* (PHENIX Collaboration), Phys. Rev. Lett. **98**, 172301 (2007).

[27] Z. Donko, J Goree, P. Hartmann and K. Kutasi, cond-mat/0603667 (2006).

[28] L.P. Csernai, J.I. Kapusta and L.D. McLerran, Phys. Rev. Lett. **97**, 152303 (2006).

[29] F. Arleo and D. d'Enterria, Phys. Rev. D **78**, 094004 (2008).

[30] U. Heinz and A.Kuhlman, Phys. Rev. Lett. **94**, 132301 (2005).

[31] S. Voloshin, Private Communication.

[32] A. Kuhlman and U. Heinz, Phys. Rev. **C72**, 037901 (2005).

[33] C. Nepali, G. Fai and D. Keane, Phys. Rev. **C73**, 034911 (2006).

[34] C. Nepali, G. Fai and D. Keane, Phys. Rev. **C76**, 051902 (2007).

[35] P. Filip, R. Lednicky, H. Masui and N. Xu, Phys. Rev. **C80**, 054903 (2009).

[36] B. Alver, M. Baker, C. Loizides and P. Steinberg, arXiV 0805.4411 (2008).

[37] A. Kuhlman, U. Heinz and Y. Kovchegov, Phys. Lett. **B638** 171 (2006).